A combined field, laboratory and numerical study of the forces applied to, and the potential for removal of, bar top vegetation in a braided river.

Natasha L. Bankhead[1], Robert E. Thomas[2] and Andrew Simon[1]

[1] Cardno, PO Box 1236, Oxford, MS. 38655. USA; Natasha.bankhead@cardno.com; 662-380-1961
[2] School of Earth & Environment, University of Leeds, Leeds, West Yorkshire. LS2 9JT. UK.

ABSTRACT

Vegetation can have an important role in controlling channel planform, through its effects on channel roughness, and root-reinforcement of bank and bar materials. Along the Platte River in central Nebraska, USA, The Platte River Recovery Implementation Program (PRRIP) has been tasked with managing the planform of the river to benefit endangered species. To investigate the potential use of planned Short Duration High Flow events (SDHFs) to manage bar vegetation, this study combined several approaches to determine whether flows of up to 227 m^3s^{-1} through the central Platte River, could remove cottonwood, Phragmites and reed canarygrass stands of various ages and densities from in-channel bars. First, fieldwork was carried out to measure the uprooting resistance, and resistance to bending for each species. Second, a set of flume experiments was carried out to measure the forces exerted on the three species of interest under different flow conditions. Finally, a numerical study compared drag forces (driving) measured in the flume study, with uprooting forces (resisting) measured in the field, was carried out for each species to determine the likelihood of plant removal by SDHFs. Results showed that plants with more than a year of root growth, likely cannot be removed through drag and local scour alone, even at the 100-year recurrence interval discharge. At most, a few cottonwood seedlings could be removed from bars through drag, scour and undercutting, where rooting depths are still small. The results presented here help us further understand the positive feedbacks that lead to the creation of permanent, vegetated bars rather than mobile braided channels. As such, the findings could help inform management decisions for other braided rivers, and the combined field, flume and modelling techniques used in this study could be applied to other fluvial systems where vegetation and planform dynamics are of interest.

Keywords: vegetation management, braided planform, drag coefficients, modelling, numerical study

1 INTRODUCTION

Vegetation interacts with river dynamics and morphology by modifying flow velocities and direction, as well as changing the resistance of the bed and bank material through the presence of roots. Altering these flow and material properties can then change the balance of force and resistance in a channel, thereby affecting channel pattern (Mackin, 1956; Nanson and Knighton, 1996; Millar, 2000).
Rivers exhibit a continuum of planform with three end-members: braided, meandering and straight (Leopold and Wolman, 1957). A number of definitions of the term 'braided river' have appeared in the literature. Friedkin (1945: 16) noted that rivers are described as braided when "the channel is extremely wide and shallow and the flow passes through a number of small interlaced channels separated by bars". Combining the definitions of Lane (1957) and Leopold and Wolman (1957), a braided river can be defined as one that "flows in two or more anastomosing channels around alluvial islands" (Leopold and Wolman, 1957: 53) "presenting from the air the intertwining effect of a braid" (Lane, 1957: 88). More modern definitions distinguish braided rivers as having an unstable planform that is dynamic, versus anastomosing planforms that are fixed over time. Paola (2001: 22) stated that braiding "is the fundamental instability of streams flowing in non-cohesive material." As such, channels formed in material with little or no cohesion or vegetative stability to restrict channel widening tend to braid (e.g. Simpson and Smith, 2001).Those channels with cohesive banks (Thorne and Abt, 1993) and/or vegetation (Mosley, 2001) become progressively more sinuous (i.e. meandering) or anastomosed (Smith and Smith, 1980; Nanson and Knighton, 1996), especially if there is some base-level control.

Over the past one hundred years, the planform of the Platte River has seen a shift from a wide braided channel system, to a narrower channel with semi-permanent vegetated bars. One cause of the planform change seen in the Central Platte River has been the diversion and storage of water for agricultural, municipal and industrial uses, which has caused significant alteration of the hydrologic regime. High flows now occur less frequently, base flows have been elevated, and there has been a decrease in sediment supply (Williams, 1978; Hadley et al., 1987). Data from USGS gauge 06768000 (Platte River near Overton, NE) show that between 1920 and 2009, decadal-average annual peak flows declined from 527 m^3s^{-1} to 106 m^3s^{-1}. During that same period, episodic channel narrowing has occurred during drought periods as vegetation encroached into the active channels (Johnson, 1994). These changes in flow regime have led to the formation of semi-permanent islands and narrowing of the braided, wide and shallow channels of the Platte by 30-90% (Williams, 1978; Figure 1).

These planform changes have had a direct impact on the availability of nesting habitat for several endangered bird species, who favour sections of wide, braided channel with un-vegetated bars, so that there are long lines of sight. As a result, the Platte River Recovery Implementation Program (PRRIP) was initiated in 2007 and tasked with managing the central Platte River to provide benefits to the endangered whooping crane and least tern, and the threatened piping plover. The Program is evaluating competing management strategies through implementation of a rigorous adaptive management plan (PRRIP, 2006). One strategy focuses on the periodic implementation of short-duration high flow (SDHF) dam releases to scour vegetation from bar margins and tops and encourage a wide, braided planform.

Determining the effectiveness of flows for removing vegetation is a matter of quantifying the driving forces provided by the flow acting on the channel boundary (predominantly sand and gravel, but modified by drag associated with any above-ground biomass), and the resistance of the boundary as modified by the additional resistance provided by roots and/or rhizomes. The driving force acting on a plant is controlled by the flow depth and velocity, the drag coefficient of the plant species being studied, and the flexibility of the plant. Measurement of these above-ground vegetation properties allows for calculation of the force being applied to the below-ground structures that act to anchor the plant into the substrate. The resisting force afforded by a plant is controlled by the tensile strength of the plant roots, stems (and rhizomes where applicable), the geometric properties of the roots (e.g. root diameter and maximum rooting depth), and number of roots, which vary by age and species. These data, along with substrate properties, can then be used to model the range of plant resistances that might occur within a given reach of the river. Where the driving force acting on a given plant, or patch of plants, exceeds the resisting force provided by the roots or stems of the same plant, or patch of plants, vegetation removal will be initiated.

It follows that for a plant to be removed from its substrate either: 1. the roots, rhizomes and/or stems of the plant must be snapped or pulled from the substrate by the force acting on the above-ground part of the plant by the flow of water or ice; or 2. the sediment surrounding the roots of the plant must be scoured sufficiently by water or ice for the plant to simply be washed away (Edmaier et al., 2011). As the force required to remove a plant from its substrate changes over time according to rooting and/or burial depth (Ennos, 1990; Pollen-Bankhead et al., 2010), the driving force required to remove a particular plant from its substrate may actually occur at some point along the continuum between these two alternatives (Figure 2), with the depth of scour required for plant removal being dependent on the local properties of the substrate and the properties of the roots of the plant in question.

The concept of SDHF as a management action for the Central Platte River was developed in the early 2000s when cottonwood and willow were generally accepted to be the species responsible for channel narrowing (Johnson, 1994). Subsequently, several exotic invasive species, including Phragmites australis and reed canarygrass have become established in the central Platte River. The present research was initiated to inform PRRIP of the likelihood of SDHF to scour colonized vegetation as well as help the PRRIP understand the implications of newly invading species like Phragmites. To investigate the various driving and resisting forces affecting plant removal, we developed a study utilizing a combination of: 1) fieldwork to measure the resistance of individual plants/stems to uprooting and bending (resisting force); 2) Monte Carlo simulations using the RipRoot model (Pollen and Simon, 2005; Pollen, 2007; Thomas and Pollen-Bankhead, 2010) to calculate resistance of patches of plants of varying densities to uprooting; 3) flume experiments to measure the drag force acting on the different plants (driving force); and 4) calculations of local scour around vegetation stems and the effect of this on the balance between the driving and resisting forces. Finally, the four strands of the study were brought together to determine whether SDHFs of up to 227 m^3s^{-1} over three days, were likely to lead to vegetation removal through scour and drag forces alone, or whether mechanical removal of vegetation will be necessary to clear bars and improve habitat.

2 QUANTIFYING DRIVING AND RESISTING FORCES ACTING ON VEGETATION: THEORY

2.1 Driving forces

In recent years, a significant amount of work has been undertaken to study the interaction between immersed vegetation and the water around it (e.g. Li and Shen, 1973; Petryk and Bosmajian, 1975; Bertram, 1984; Pasche and Rouvé, 1985; Fathi-Moghadam and Kouwen, 1997; Nepf, 1999; Freeman et al., 2000; López and García, 2001; Bennett et al., 2002; Stone and Shen, 2002; Järvelä, 2002; 2004; Wilson et al., 2003; 2006; McBride et al., 2007; White and Nepf, 2008). Submerged or emergent vegetation reacts to the drag exerted by water by either remaining erect, oscillating in response to turbulent fluctuations or bending (Paul et al., 2013). The magnitude of the drag force is a function of several factors that vary by plant type and age. These factors include plant flexibility, frontal projected area, relative depth of submergence, and spatial density (Li and Shen, 1973; Petryk and Bosmajian, 1975; Pasche and Rouvé, 1985; Fathi-Moghadam and Kouwen, 1997; Nepf, 1999; Freeman et al., 2000; Bennett et al., 2002; Stone and Shen, 2002; Järvelä, 2002; 2004; Wilson et al., 2003; 2006; White and Nepf, 2008; Paul et al., 2013). As noted by Paul et al. (2013), vegetation also affects flow patterns by adding roughness and hence reducing the velocity in vegetated areas, introducing turbulence and inducing scour along the vegetation-channel interface, and forcing flow back towards

the open channel (Bertram, 1984; McBride et al., 2007; White and Nepf, 2008). Vegetation can also have a protective role, reducing bank erosion in rivers, estuaries, lakes and coastal zones through deflection of flow away from banks (White and Nepf, 2008; Hopkinson and Wynn, 2009), dissipation of wave energy (Moller et al., 1999), and reinforcement of the soil matrix by plant roots (Pollen and Simon, 2005; Thomas and Pollen-Bankhead, 2010).

Most researchers commence the estimation of drag forces with consideration of the fundamental equations describing the time-averaged turbulent flow of an incompressible fluid (Equation 1; López and García, 2001; Paul et al., 2013). For a unit volume of water, the change in fluid momentum in all three directions is balanced by the gravitational force acting on that unit volume of water:

$$\frac{\partial}{\partial x}\left(\mu\frac{\partial \bar{u}}{\partial x}-\rho\overline{u'}\right)+\frac{\partial}{\partial y}\left(\mu\frac{\partial \bar{u}}{\partial y}-\rho\overline{u'v'}\right)+\frac{\partial}{\partial z}\left(\mu\frac{\partial \bar{u}}{\partial z}-\rho\overline{u'w'}\right)+\rho g h S_0 = 0 \quad (1)$$

where ∂ = partial differential operator, μ = dynamic viscosity of water (~1.4×10^{-3} N s m^{-2}), ρ = mass density of water (~1000 kg m^{-3}), g = acceleration due to gravity (~9.81 m s^{-2}), h = flow depth (m), S_0 = bed slope (m m^{-1}), and u, v and w = instantaneous velocities (m s^{-1}) in the along-stream (x), across-stream (y) and vertical (z) directions, respectively. Overbars represent time-averaged values and primes refer to fluctuations about these values.

López and García (2001) argue that the first and second terms of Equation 1 are dominated by the third and fourth terms so that only those terms need to be retained (López and García, 2001):

$$\frac{\partial}{\partial z}\left(\mu\frac{\partial \bar{u}}{\partial z}-\rho\overline{u'w'}\right)+g h S_0 = 0 \quad (2)$$

Further, Equation 2 also needs to be averaged in a horizontal plane to properly represent the flow through vegetation in a one-dimensional frame (López and García, 2001):

$$\frac{\partial}{\partial z}\left(\mu\frac{\partial U}{\partial z}-\rho\overline{U'W'}\right)-\frac{1}{2}C_D\rho A_p U^2+g h S_0 = 0 \quad (3)$$

where the uppercase U and W denote time- and space- (in a horizontal plane) averaged velocities, C_D = dimensionless drag coefficient, and A_p = frontal area of vegetation per unit volume of fluid (m^{-1}).

This averaging process has, therefore, introduced additional parameters into Equation 3 (C_D and A_p) that account for the effects of vegetation:

$$\frac{F_D}{V} = \frac{1}{2} C_D \rho A_p U^2 \tag{4}$$

where F_D = drag force (N) and V = volume of fluid in which vegetation is immersed (m^3). Equation 4 may also be applied to patches of vegetation by using the appropriate area and a reduced C_D value (e.g. Nepf, 1999).

Dunn et al. (1996), showed that in a one-dimensional frame of reference, Equation 3 could be further reduced (averaged over space and time), yielding a backwater curve for open-channel flow through emergent vegetation. They found that the mean drag coefficient, $\overline{C_D}$, for patches of vegetation could be estimated using:

$$\overline{C_D} = 2g \frac{S_0 - S_f - \frac{dh}{dx}\left(1 - \beta \frac{[Q/A]^2}{gh}\right)}{A_p \beta [Q/A]^2} \tag{5}$$

where S_f = friction slope estimated using Manning's equation, Q = flow discharge ($m^3 s^{-1}$), A = flow area (m^2) and β = a coefficient accounting for the vertical distribution of the streamwise velocity, estimated by vertically integrating multiple measurements of the squared ratio of U to the depth-averaged velocity (Dunn et al., 1996).

Because plants growing on the semi-permanent bars in the central Platte River are commonly found in patches, Equation 5 is particularly pertinent to this study.

2.2 Resisting forces

The force required to remove a plant from its substrate before the entire root ball has been scoured out by water or ice is a function of a number of variables, including the number of roots, the strength and diameter distributions of those roots, and the orientation of those roots (Wu et al., 1979; Waldron and Dakessian, 1981; Greenway, 1987; Gray and Sotir, 1996; Simon and Collison, 2002; Pollen and Simon, 2005; Pollen-Bankhead and Simon, 2009). The elastic (Young's) moduli of the roots, antecedent soil and root moistures, and frictional forces between the soil and roots have also been shown to be important (Pollen, 2007; Fan and Su, 2008).

There are two mechanisms by which current drag can directly remove a plant from its substrate: by stem or root rupture, or by pullout. In simplest terms, the force required to break an individual root is given by:

$$F_b = A_r T_r \quad (6)$$

where F_b = root breaking force (N), A_r = cross-sectional area of the root at the point of rupture (mm^2), and T_r = tensile strength of the root (MPa).

The force required to pull an individual root out of the soil without breaking is a function of the surface area of the root embedded within the soil and the cohesive and frictional resistance developed between the root and soil and can be represented by:

$$F_p = \pi D_r L_r \tau_f f \quad (7)$$

where F_p = root pullout force (N), D_r = diameter of the root (m), L_r = rooting depth (~length) of the root (m), f is the dimensionless coefficient of friction between soil and wood, which ranges from 0.7 to 0.9 (Potyondy, 1961; Gray and Sotir, 1996: 82), and τ_f = shear strength of the soil (Pa), given by (Fredlund et al., 1978):

$$\tau_f = c' + (\sigma - \mu_a) \tan \phi' + (\mu_a - \mu_w) \tan \phi^b \quad (8)$$

where c' = effective cohesion (Pa), σ = normal force acting on the outside skin of the root (Pa), μ_w = pore-water pressure (Pa), ϕ' = effective angle of internal friction (°), μ_a = pore-air pressure (Pa), and ϕ^b = angle representing the increase in shear strength for an increase in matric suction (°).

Equations 6 and 7 quantify the forces required to either break or pullout an individual root, but to correctly model the reinforcement provided by an entire root ball or root bundle, we must also consider the mechanism by which a force is applied to, and distributed amongst, multiple rather than individual roots. The present work applies a progressive breaking algorithm developed from the fiber bundle models of the materials sciences (Daniels, 1945; Hidalgo et al., 2001). Fiber bundle models work by apportioning the total load applied to a bundle of fibers and then monitoring whether the load applied to a fiber exceeds its strength. In the RipRoot model developed by Pollen and Simon (2005) and Pollen (2007), when a load was applied to the root ball, it was apportioned equally between all the intact roots. The maximum load that could be supported by the root ball corresponded not to the weakest or strongest root, but to one of the roots in the middle (Thomas and Pollen-Bankhead, 2010).

RipRoot was validated using direct-shear tests of soils permeated with various densities of switchgrass roots (Pollen and Simon, 2005), and was shown to provide much more accurate comparisons to measured data than existing approaches (e.g. Wu et al., 1979).

To account for some of the remaining inaccuracies, Pollen (2007) included root pullout as an alternative failure mechanism. In this approach, it was assumed that the normal force acting upon the outside skin of roots was zero and that all soil strength was due to effective cohesion and matric suction. Pullout was shown to be particularly important for shorter roots and in soils with lower cohesion (Pollen, 2007), such as those with a high sand content like the Platte River. Thomas and Pollen-Bankhead (2010) included the effects of friction between the root and the soil by computing the normal force using Rankine's active earth-pressure theory (Terzaghi and Peck, 1967: 193-200). In addition, Thomas and Pollen-Bankhead (2010) used RipRoot in a Monte Carlo simulation framework in order to model potential variability in root diameter distributions, root lengths and root orientations. Monte Carlo simulations hence provide a mechanism by which to test and validate the sensitivity of the various input parameters and to reduce uncertainty in predicted erosion thresholds.

Since the publication of RipRoot by Pollen and Simon (2005), the progressive breaking algorithm such as the one used in the RipRoot model has become the method of choice for many studies of root-reinforcement (e.g. Docker and Hubble, 2008; Loades et al., 2009; Mickovski et al., 2009; Schwarz et al., 2010). Although the model was originally developed for use with slope and streambank stability models, the model output provides the maximum load that can be supported by a given number of roots. In the case of plant removal from a substrate, the maximum load the roots of a given plant are predicted to be able to support can be directly compared to the force that is applied to that plant by the flowing water. This provides the threshold driving force required to exceed the resisting force. The RipRoot model has previously been used by the authors in a similar study of plant removal processes for the invasive species Sparganium erectum (Pollen-Bankhead et al., 2011; Liffen et al., 2011).

3 QUANTIFYING DRIVING AND RESISTING FORCES ACTING ON VEGETATION: METHODOLOGY

3.1 Study Sites

Fieldwork was undertaken at a range of sites on the Platte River that were populated with Phragmites australis, up to 2 year old cottonwood seedlings (Populus deltoides), and reed canarygrass (Phalaris arundinacea) (Figure 3). The areal density of each plant species (number of stems per unit planform area) was surveyed in five different locations to inform flume experiments used to quantify the

driving (drag) force and also for input to the RipRoot model to quantify the resistance to pullout of patches of plants of different areal densities. Testing and measurement protocols specific to the quantification of either the driving or resisting forces are detailed in the following sections. Field measurements were taken in July, at the peak of the growing season. Timing of measurements could affect the bending forces of the plants, (depending on damage from spring floods and/or wind) and could also affect pullout forces. The peak of the growing season was selected so that maximum root growth for that season would be measured.

3.2 Measuring Driving Forces

As described previously, the magnitude of the driving (drag) force acting upon the stem of a plant is a function of plant flexibility, frontal projected area, relative depth of submergence, and density (Li and Shen, 1973; Petryk and Bosmajian 1975; Pasche and Rouvé, 1985; Fathi-Moghadam and Kouwen, 1997; Nepf, 1999; Freeman et al. 2000; Bennett et al., 2002; Stone and Shen 2002; Järvelä 2002; 2004; Wilson et al., 2003; 2006; White and Nepf 2008), which may all vary by species and age. Quantifying the drag force is complicated by the fact that both the frontal area and the drag coefficient may vary depending upon the flexibility of the plant (which will vary by species and may also vary temporally), extent of submergence and the flow velocity, U. A coupled field and laboratory methodology was adopted here to quantify the drag force. First, a specially-designed and constructed apparatus was used to simultaneously monitor the angle to which the stem of a plant has been bent, the force required to bend that stem, and the resulting frontal area in a series of field tests. Second, a series of laboratory flume experiments were designed to estimate the drag coefficient of plant stems at different flow depths and velocities.

3.2.1 Field protocol to measure bending forces

To assess the extent to which a given force could bend the stem of a plant and cause it to streamline, an apparatus was designed to apply a known horizontal force to the stem, continuously monitor the distance the stem had been displaced and quantify the amount of streamlining (reduction in frontal area). The apparatus (Figure 4) consisted of:

1. A lightweight load cell, calibrated in tension, affixed at a height of approximately ⅓ the height of the plant. This height was selected as it represents the maximum pulling force related to the assumed depth of flow;
2. A high-capacity reel spooled with high tension line graduated at 25 mm increments fixed to a telescopic arm that could be adjusted to ensure horizontal loading. The telescopic arm was welded to a specially-designed mount to prevent toppling or sliding of the apparatus;
3. A 12 MP camera fixed on a tripod at the same elevation and horizontal distance from the stem as the reel; and

4. A blue screen placed behind the vegetation to facilitate automated identification of the vegetation on images in order to estimate the frontal area of the plant.

At each stem displacement, the applied load was noted and an image captured. For each species and age range, at least 20 plants were selected for testing and the external and internal (where appropriate) stem diameters and lengths were measured.

The collected data were used to determine the flexibility of vegetation, represented by Young's modulus of elasticity (E), with:

$$E = \frac{J}{I} = \frac{F_D L}{48 \delta I} \quad (9)$$

where E = Young's modulus of elasticity (N m^{-2}), J = flexural stiffness (N m^2), I = second moment of inertia ($I = \pi D_s^4/64$, in m^4), D_s = stem diameter (m), δ = deflection of the stem (m), and L = stem length (m).

3.2.2 Laboratory flume experiments: measuring driving and drag forces

A series of laboratory flume experiments were designed to permit the estimation of the drag coefficient (using Equation 5). Although both artificial and natural flexible woody vegetation have been used in some studies to determine the value of resistance coefficients (Fathi-Moghadam and Kouwen, 1997; Freeman et al., 2000; Järvelä , 2002; Wilson et al., 2006), most flume experiments of stream channels use woody vegetation in the simplest form, represented as wooden dowels or similar rigid structures (Pasche and Rouvé, 1985; Bennett et al., 2002; McBride et al., 2007; White and Nepf, 2008). Herein, artificial materials were selected to mimic field-measured mean-stem diameters and flexural stiffnesses (Figure 5).

Field tests showed that the mean flexural stiffness of cottonwood seedlings was 0.0099 ± 0.0082 N m^2 (mean ± 1 standard deviation, number of tests = 10, number of evaluations = 23), that of 3-5 year old cottonwoods was 1.53 ± 1.86 N m^2 (number of tests = 10, number of evaluations = 80), that of Phragmites was 0.94 ± 1.07 N m^2 (number of tests = 21, number of evaluations = 105), and that of reed canarygrass was 0.18 ± 0.17 N m^2 (number of tests = 16, number of evaluations = 62) (Table 1). The relative magnitudes of the means and standard deviations highlight the variability in J-values and the positive skewness of their distributions. For this reason, J-values were verified by plotting the computed flexural stiffness values against the stem diameter-length ratios and then finding the flexural stiffness associated with the mean stem diameter-length ratio. For both reed canarygrass and cottonwood seedlings, the resulting flexural stiffness was not statistically different than the computed mean flexural stiffness, but for Phragmites, the computed mean flexural stiffness was 0.25 N m^2. As

the stems of Phragmites displayed similar behaviour to those of reed canarygrass in the field, this value was selected as the target value for artificial material selection to be used in the flume experiments. For similar stem diameters, a survey of available materials from a number of manufacturers and suppliers identified fiberglass rods, acrylic tubes, and polypropylene rods as having almost identical flexural stiffnesses (0.0087, 0.24, and 0.21 N m^2) to those of cottonwood seedlings, Phragmites, and reed canarygrass, respectively.

Artificial cottonwood "plants" were constructed with four "leaves" made of contact paper and attached to the stem with fishing line "branches" to mimic the flexibility, size and roughness of real cottonwood leaves observed in the field (mean breadth at widest point = 40 mm ± 12 mm, mean length = 45 mm ± 2.7 mm, mean area of 1350 mm^2 ± 291 mm^2, n = 10; Figure 5 inset). The addition of leaves to the cottonwood plants was deemed necessary because the resistance behaviour of rigid elements compared to foliated vegetation has been shown to be significantly different in several previous studies (summarized in Aberle and Jarvela, 2013). The stem of each artificial cottonwood plant was 0.30 m long (field values = 0.38 ± 0.09 m, n = 63) and had a diameter of 3.18 mm (field values = 2.92 ± 1.38 mm, n = 66); leaves 1 and 2 were attached 5 mm from the top, leaves 3 and 4 were attached 55 mm from the top. For Phragmites and reed canarygrass, only the stems were modelled (Figure 4) because it was found that leaves were generally high up on stems (and thus significant flow depths/velocities would be required to first bend them and then submerge them), and had a minimal frontal area. The fiberglass rods used to mimic reed canarygrass were 0.45 m long and had a diameter of 3.18 mm (field values 3.21 ± 1.08 mm (mean ± 1 standard deviation, number of tests = 69). The acrylic tubes used to mimic Phragmites were ~0.40 m long (± 0.02 m), with internal diameters of 3.18 mm and external diameters of 6.36 mm (field values = 3.27 ± 0.67 mm, n = 55 and 6.0 ± 1.94 mm, n = 91, respectively).

Flow depths and plant heights were selected so that cottonwood seedlings were submerged during the experiments, whereas the reed canarygrass and Phragmites were emergent, with the top of the stems just out of the water. This was based on flow depths estimated using a rating curve developed for the USGS gauging station near Kearney (USGS 06770200), which suggested that for a 227 m^3s^{-1} event, flow depth should be about 0.4 m over the bar tops. Artificial plants were installed in a 6.05 × 0.61 × 0.61 m recirculating flume at areal densities matching those observed in the field. In the case of cottonwoods, because they were distributed relatively sparsely, five different randomly-generated configurations were installed. It was important to replicate stem densities measured in the field because as noted earlier, a group of obstructions such as plant stems can behave as a "patch", influencing each other and flow velocities, drag coefficents and sediment transport characteristics measured within and around them (Tanino and Nepf, 2008; Zong and Nepf, 2010).

Experiments were run using a fixed slope of 0.001 m m^{-1} to approximate central Platte River slope (Simons and Associates Inc., 2000), two different flow rates (0.029 m^3s^{-1} and 0.048 m^3s^{-1}, respectively) and three different weir heights (0.30, 0.35 and 0.40 m, respectively). Flow velocities in the flume study reached a maximum of 0.25 m s^{-1} due to the physical restrictions of the flume itself, whereas velocities in the Platte River during a SDHF event could be expected to reach 1.5 m s^{-1}. The drag forces and exponents calculated from these experiments were, therefore, extrapolated to attain values for the full range of potential field conditions. This is discussed later. An example of the flume set up for a Phragmites run is shown in Figure 5. To dampen turbulence and provide uniform flow, water was passed through a rock damper and an array of 0.30 m long, 0.02 m diameter tubes (baffles). Water surface elevations were measured over a 0.2 m grid using a point gauge. Ultrasonic Doppler Velocity Profilers (UVPs) were used to record high precision directional velocity data across the entire flow field. Ten transducers were multiplexed (where each transducer records a profile in turn), so that while each profile took up to 18×10^{-3} s to record, they were separated by a 15×10^{-3} s delay between transducers, yielding a total sampling time of up to 33×10^{-3} s (Table 1). The delay ensured that there were no echo effects or "cross talk" between the transducers, resulting in a data capture rate of approximately 40 Hz.

For the no vegetation case, streamwise velocities were sampled on horizontal planes spaced 0.05 m apart, starting 0.05 m above the bed, i.e., 0.05, 0.10, 0.15, 0.20, and 0.25 m above the bed for the 0.30 m weir and with additional planes added for higher weir heights. By combining data from all the profiles, it was then possible to establish the vertical variations in streamwise velocity at a specific along-stream coordinate. For the vegetated cases, streamwise velocity profiles were taken on horizontal planes spaced 0.10 m apart, starting 0.10 m above the bed, i.e., 0.10 and 0.20 m above the bed for the 0.30 m weir, and again adding additional planes for higher weir heights.

3.3 Measuring Resisting Forces

Much of the work to quantify root strength has been conducted to assess potential changes in slope and streambank stability with different types and ages of vegetation (e.g., Greenway, 1987; Coppin and Richards, 1990; Gray and Sotir, 1996; Simon and Collison, 2002; Bischetti et al., 2005; Pollen and Simon, 2005, Simon et al., 2006; Pollen, 2007; Tosi, 2007; Danjon et al., 2008; De Baets et al., 2008; Docker and Hubble, 2008; Hales, 2009; Pollen-Bankhead and Simon, 2009; Thomas and Pollen-Bankhead, 2010). In the present study, existing protocols that had been established to quantify the geometric properties and strengths of roots were supplemented with new protocols to quantify the relative strengths of stems, roots and rhizomes. The latter were required to identify whether it was

possible to remove entire plants intact, or whether a particular plant structure would break preferentially before removal.

3.3.1 Field protocol: Root tensile strength measurement

At each study site, plants of each species were excavated by carefully exposing their root architectures to enable the measurement of typical rooting depths. Root tensile strengths were then measured using a device called the Root-Puller, based on a design by Abernethy and Rutherford (2001) (Figure 6A). This comprised a metal frame with a winch attached to a load cell and connected to a data logger. Different diameter roots were then tested by securing each individual root in a U-bolt that was then connected to the load cell. Cranking the winch applied tensile stress to the root (measured as a load, in N) that increased until tensile failure of the root occurred. The diameter of each root was recorded along with the logged history of applied force until breaking. The maximum load applied to each root before breaking and the root diameter was then used to calculate the ultimate tensile stress of each root. A sample size of >30 roots, was collected to establish a relation between root diameter and root tensile strength, and in the case of Phragmites, to establish a rhizome diameter-tensile strength relation. The tensile strength of roots commonly varies inversely with root diameter, as a non-linear trend typically of the form $T_r = aD_r^{-b}$ (e.g., Waldron and Dakessian, 1981; Riestenberg and Sovonick-Dunford, 1983; Greenway, 1987; Coppin and Richards, 1990; Gray and Sotir, 1996; Abernethy and Rutherfurd, 2001; Simon and Collison, 2002; Pollen and Simon, 2005; Genet et al., 2006; De Baets et al., 2008; Fan and Su, 2008; Hales et al., 2009; Thomas and Pollen-Bankhead, 2010).

3.3.2 Field protocol: Plant removal tests

The methods outlined in section 3.3.1 permitted the quantification of the geometric properties and strengths of roots, but did not identify whether a particular plant structure (i.e., stem, root or rhizome) would break preferentially before removal, nor quantify the load required to break (or pullout) an entire root-ball. To this end, a new apparatus was designed and constructed. This apparatus comprised a tripod, winch and load cell, placed above each plant stem (Figure 6B). The stems of individual plants were attached to the load cell and the plant winched vertically upwards, thereby measuring the force required to remove the entire root ball from its substrate. The plants were pulled vertically because the force required to break a root or break the soil-root friction bond is independent of the direction the plant is pulled in, and pulling the plant vertically ensured that the measured force was a function simply of the uprooting force, without a stem bending component. The forces required to remove plants of each species were measured during two fieldtrips, along with corresponding stem diameters. After each plant was removed, or the stem snapped, the failure mode was recorded (pullout, stem breaking, roots/rhizomes breaking) and the maximum rooting depth and lateral rooting extent was measured. Digital images of each root network were also captured, so that intact root networks could be analyzed using the WinRhizo software to quantify total root length, root volume

and root surface area. Lastly, substrate samples were taken at each study site to test for variations in bulk unit weight, moisture content and particle size.

3.3.3 Numerical modelling: root network resistance to removal

Field measurements of whole plant removal will likely yield a relatively small sample size that only represents part of the population of plant resistances that are actually present in a given reach. To account for parameter variability and to estimate the full range of plant resistances to removal, the RipRoot model was executed within a 25,000-run Monte Carlo framework (modified from Thomas and Pollen-Bankhead, 2010). Field measurements provided the data necessary to parameterize simulations for the three species investigated in the present study. For each species, the measured minimum and maximum numbers of roots per plant, minimum and maximum root diameters, tensile strength-diameter curve, and the range of typical rooting depths (obtained from direct measurements and from the images of extracted plant networks) were used as input to the model (Table 2). RipRoot results for uprooting forces of individual plants, calculated using the input data described in Table 2 (from individual roots and rhizomes), were compared to the plant pullout dataset collected in the field to ensure they were within the same range, before extending the simulations to patches of plants. To model patch resistance to pullout, plant areal densities (number of stems per unit planform area) were added to RipRoot as an additional variable. Average substrate bulk unit weight (19.2 kN) and friction angle (27°) were determined from samples collected at the field sites. In all of the RipRoot simulations, soil cohesion was set to be 1 kPa to be representative of the sand and fine silt substrate that would most likely be present during a SDHF event.

RipRoot modelling provided predictions of mean plant and patch resistances, with upper and lower bounds for:

1) Different species;
2) Different ages of each species where applicable;
3) Different densities of plants growing on a given bar; and
4) Different depths of burial and scour.

4 RESULTS

4.1 Drag coefficients and drag forces

Drag coefficients (C_D), were computed using data collected during the laboratory flume experiments and Equation 6 (Table 3). At low discharge (0.0285 m^3s^{-1}), drag coefficients were found to vary from 8.81 to 26.1. At high discharge (0.0478 m^3s^{-1}), drag coefficients were found to vary from 7.27 to 21.1. These values are high relative to those reported previously (e.g., García et al., 2004 for a discussion),

although they are similar to those reported by James et al. (2008), who studied drag forces on Phragmites for a variety of submergences and velocities. James et al. (2008) noted that C_D-values are sensitive to the method used to characterize the projected area, and Li and Shen (1973), noted that errors in computing projected area values would result in higher mean drag coefficients. Of interest is the finding that the drag coefficient acting upon artificial cottonwood seedlings displays the opposite trend to that on both artificial Phragmites and artificial reed canarygrass: for constant areal densities and discharges, shallower flow depths yielded smaller drag coefficients than deeper flow depths. In other words, higher velocities yielded smaller drag coefficients. This confirms that streamlining is important in limiting drag on cottonwood seedlings, because the reduction in velocity (U), is approximately balanced by the reduction in projected area. This conclusion is reinforced by comparing the drag coefficients obtained when varying discharge for constant areal densities and weir heights (Table 3). Conversely, both artificial Phragmites and artificial reed canarygrass were stiff enough that their projected areas did not change during the flume experiments and therefore for constant areal densities and discharges, drag was larger at shallower flow depths and faster velocities.

Using Equation 4 with the computed drag coefficients (C_D), and projected areas, the drag forces acting upon the artificial plants can be computed (Table 3). At low discharge (0.0285 m^3s-1), drag forces were found to vary from 1.02 to 2.16 N and at high discharge (0.0478 m^3s^{-1}), drag forces were found to vary from 1.67 to 5.00 N. These values are commensurate with those obtained by previous researchers. For example, Schnauder and Wilson (2009) assembled datasets obtained by a number of researchers and showed that drag forces acting on various willow species ranged from 0.5 to 12 N for the range of flow velocities measured herein.

A number of trends are evident in our experimental results. First, in all cases, for a given discharge the drag force is higher for shallower flow depths and faster velocities. Second, in all cases, for a given flow depth, the drag force is higher for larger discharges and faster velocities. Third, in all cases, for a given species, the drag force is higher for larger areal densities (stems m^{-2}). Fourth, the drag force acting upon the stand of artificial Phragmites plants with an areal density of 200 stems m^{-2}, is almost identical to that acting upon the stand of artificial reed canarygrass plants with an areal density of 400 stems m^{-2}. This is because the stem diameter of the artificial Phragmites plants is exactly double that of the artificial reed canarygrass plants. The projected areas of these two cases are therefore identical.

4.2 Root architecture

Excavation of the plant species included in this study revealed rather different root architectures and extents (Figure 7). Reed canarygrass exhibited a very dense, fibrous root network that extended to approximately 0.5 m deep in places, with most roots in the upper 0.3 m of the soil profile (Figure 7A). Root densities were of the order of tens of thousands of roots m^{-2}, ranging from 0.1 to 2 mm in diameter.

Young cottonwood seedlings (up to 2-years) had a much sparser root network, composed of roots that were more woody in texture (Figure 7B). The one-year old seedlings had already developed a distinct, woody taproot that extended up to 0.25 m into the soil profile, with a mean rooting depth of 0.14 m. Smaller, lateral roots extended from the upper portion of the taproot to assist in anchoring. For two-year old seedlings the maximum rooting depth measured was 0.48 m, but again the mean rooting depth was 0.14 m. Several five-year old cottonwoods were also excavated to see how development continues over the next few years of growth. The taproot continued to dominate the root architecture, extending up to 1.5 m in some cases, or to whatever depth was necessary for the plant to reach sufficient moisture. These trees therefore exhibit rapid taproot growth over the first few years of their development, which has important implications for the timing of any potential removal of these trees, be it by mechanical or hydraulic means.

Phragmites stands tended to be dominated by interconnected networks of rhizomes, with fine roots growing from them (Figure 7C). Excavation revealed deeply rooted rhizomes, extending to depths of greater than 1.5 m in places. Even where stands of Phragmites had been sprayed, the buried rhizome networks seemed healthy and capable of regenerating above-ground biomass in the following growing season. Rhizomes were even seen to have grown vertically through the soil profile from buried old stems of Phragmites. Each individual stem of Phragmites had a rhizome, commonly 10 mm or more in diameter, with multiple fibrous roots growing at nodes along the rhizomes. As the most deeply rooted plant studied, and the plant with the greatest ability to regenerate from buried rhizomes and stems, it is likely the hardest of the studied species to remove from sandbars in the Platte River.

4.3 Root and rhizome strengths

Root and rhizome strengths varied considerably between the species studied. The reed canarygrass roots tested were 1 mm in diameter or less, and exhibited very low breaking forces of up to just 5.60 N (Figure 8). These low breaking forces help to explain why during uprooting tests, the reed canarygrass stems almost always broke right at the base of the stem where root growth had initiated; even though many roots grow from each stem, the force required to break all of the roots was still less than was required to break the stem, or to pull the roots out of the ground intact. Phragmites roots and rhizomes required breakage forces of up to 456 N (Figure 8). Although the maximum breakage force measured for cottonwood roots was 398 N (Figure 8), these were actually the strongest roots of the three species tested when comparing roots of the same diameter (as indicated by the regression line with the steepest gradient in Figure 8, indicating that for a root of the same diameter, a greater force was required to break a cottonwood root than a Phragmites root/rhizome or a reed canarygrass root). The strength of the cottonwood roots helps to explain why entire root networks of cottonwood seedlings were extracted from the soil during uprooting tests; the force required to pull them out of the soil was less than the force that would have been required to break them. Statistical analyses (Kruskal-

Wallis one way analysis of variance on ranks) showed that the differences in the median root breaking forces of the three species were greater than would be expected by chance and that there is, therefore a statistically significant difference between all three data sets ($P<0.001$).

4.4 Plant resistance to pullout

In this section we discuss the range of forces measured in the field that were required to remove individual plants of each species from their substrates, and the dominant failure modes seen for each species during pullout tests. Tests were conducted in October, at the end of the growing season, but before full die back of fine root biomass for the winter months. As such, uprooting forces measured at this time should represent values in the upper range of those possible over the course of a year, with lowest uprooting forces occurring in winter months, and highest values occurring in late summer when fine root biomass and rhizome extent are at their greatest.

The one-year old cottonwood seedlings (or seedlings in their first year of growth) had the lowest removal forces, ranging from 8.2 to 64.3 N (mean value = 32.0 N, st. dev. =13.8; sample size n = 50) (Figure 8). In each test, the plant was removed smoothly as the stem was winched upwards, no breaking was heard, or any evidence of breaking seen when each plant root network was examined. Plant root networks were, therefore, considered to have been extracted intact. It is hypothesized that this was enabled by the simple taproot-dominated structure of the root network. The two-year old cottonwood seedlings required greater force for removal, ranging from 6.4 to 474 N (mean value = 139 N, st. dev. = 96.0; sample size n = 30) (Figure 8). Similar to the one-year old seedlings the majority of the root network of each plant was removed during each test, but in some cases the main taproot showed evidence of breakage. The greater number of lateral roots and their increased surface area both increased the force required to remove the plant in these vertical uprooting tests. Statistical tests (Mann Whitney rank sum) showed that a significant difference existed between the median values for uprooting of one and two-year old cottonwoods ($P<0.001$). One- and two-year old cottonwood uprooting forces were also found to be statistically significantly different from those measured for reed canarygrass, and Phragmites (Mann Whitney rank sum; $P<0.001$).

Resistance to removal for reed canarygrass stems ranged from 2.5 to 192 N (mean value = 58.3 N, st. dev. = 31.5; sample size n = 100). In almost all uprooting tests for this species, failure of the stem occurred right at the base of the stem where the roots initiate. The fibrous roots of reed canarygrass were dense and highly connected, but each individual root was small and easy to break. In some tests a short length of root was extracted from the substrate, but there was always evidence of root rupture, with the majority of roots thus being left in the ground.

Phragmites stems required the largest uprooting forces out of the four species tested. Forces required for failure of the Phragmites stems ranged from 8.9 to 740 N (mean value = 255 N, st. dev. = 151; sample size n = 115; Figure 8). Statistical tests showed that the median value of the uprooting forces for Phragmites was significantly different than all the other species tested (Mann Whitney rank sum; $P<0.001$). The large range of values is likely due to sampling a range of stem ages and diameters. During uprooting tests for this species, the part of the plant that most often failed was the main rhizome attached to each stem, indicating that when pulling on the plants, each stem was stronger than its rhizome. It was interesting to note, however, that the rhizomes were rarely pulled from the ground intact, with visible and audible signs of breakage in almost every test. This indicates that even when the force applied to Phragmites stems is great enough to cause the rhizome to break, parts of the rhizome network will still be left in the ground, and the plant will thus be able to regenerate in following growing seasons. A few dead Phragmites stems that had been sprayed were also tested for pullout resistance. These stems were very brittle and broke easily at the soil surface, leaving the root and rhizome networks in the substrate.

4.5 RipRoot modelling of individual plants and plant patches

Plant dynamics on a vegetated bar are determined not only by the characteristics of individual plants, but also by patch dynamics. To model pullout forces for different densities of plants, the RipRoot model was first validated using the field data collected for individual plants. To model each species, the species-specific failure mechanisms noted in the field were applied to the RipRoot code. In the cases of Phragmites and reed canarygrass, the code was modified so that breaking was the only root/rhizome failure mechanism, whereas for the cottonwood seedlings the code was left unmodified so that pullout or breaking could be calculated in the model using the diameter of the roots and the frictional strength of the substrate material; for each modelled root or rhizome, the model then selected the mechanism with the lesser force. Comparing the modelling results with the field data collected for the Platte River, NE, we found that the model estimated the range of potential uprooting forces well for each species when the correct root failure mechanism was accounted for.

Once RipRoot had been validated against field data for individual plants, additional Monte Carlo simulations were performed to quantify the range of potential patch resistances for each species. Minimum and maximum stem densities measured on bars of the Central Platte River were used as input to the model, along with minimum and maximum numbers of roots/rhizomes per stem. The model then selected a diameter for each root/rhizome, based on minimum and maximum values for each species measured in the field, and calculated individual tensile strengths, based on species specific relationships obtained during fieldwork. The algorithm then grouped and sorted the

roots/rhizomes from each stem to run the progressive breaking algorithm. For each species, 25,000 runs were carried out to establish a range of patch resistances for each species.

The modelled resistance of a patch of plants was dependent on the number of roots per plant, the strength of those roots, and the number of plants per planform area. RipRoot results for patch resistances showed dramatic differences between the three species. Patches of cottonwood seedlings had the lowest patch resistances, ranging from 0.4 (sparse seedling density) to 685 N (highest seedling density) for 1-year old seedlings and from 0.7 to 2,400 N for 2-year old seedlings. Reed canarygrass had the next highest patch resistance to uprooting, with forces ranging from 2.7 to 8,500 N. Phragmites had by far the highest resistance to uprooting, with estimated forces ranging from 300 to 42,000 N.

An important result of these simulations was that the range of uprooting resistances for individual plants predicted by RipRoot was slightly larger (in terms of minimum and maximum forces) than the range of measured values in the field. As noted in the methodology, up to 100 plants per species were measured in the field, and these values, along with additional input data measured in the field were used to parameterize the model. When the model was run, 25,000 iterations were performed, resulting in a larger range of output values than that given by the field data; this RipRoot output range reflected the potential upper and lower limits of plant resistances that could have been expected had our sample size in the field been significantly larger. The implications of these patch resistance results in terms of plant removal by flowing water will be discussed in Section 5 when these forces are compared with the drag forces.

5 DISCUSSION: IMPLICATIONS FOR THE MANAGEMENT OF VEGETATION

In the previous sections we have provided the drag forces acting on each of the three plants species during flume experiments, and the in-field measurements of resistance of the same species to uprooting and bending. In this section, we will draw together those results to evaluate whether Short Duration High Flow events (SDHFs) of 142 to 227 m^3s^{-1} are likely to be of sufficient duration and magnitude to remove stands of those species. In addition, we will discuss predicted values of local scour around plant stems for a range of discharges, and the effect that local scour may have on plant removal alone and in combination with drag forces.

5.1 Comparing drag forces (driving) with uprooting forces (resisting) of vegetation

For plants to be removed from their substrate (in this case mid-channel and lateral bars) during a flow event, the driving forces acting on the vegetation must exceed their resisting forces. To illustrate how these forces compare, Figures 9-11 show the minimum, maximum and mean modelled patch resistance values and measured bending resistance values for the three species tested herein (cottonwood seedlings < 2 years old, Phragmites, and reed canarygrass). The statistical distribution of plants within these ranges is unknown and is expected to vary according to site-specific variations such as water table height, local plant competition, and substrate composition. In each figure, two horizontal lines indicate where the drag forces (driving) overlap with the resisting forces (uprooting or bending). The first line shows the highest drag force measured for up to 0.25 m s^{-1} flow velocities measured in our flume study, and the second line shows the estimated increase in drag forces that could be expected for velocities that could be expected during a SDHF event on the Platte River of up to 1.5 m s^{-1}. Extrapolation of the flume velocities to higher field velocities was acheived by using Equation 4, in combination with the laboratory derived drag coefficients from Section 4.1. An iterative solver was used to solve for the applied force and the projected area for a given velocity. In the flume study performed here, drag coefficients did not vary greatly with discharge (two discharges were tested in the flume, the largest of which was double the smaller one), so it was deemed acceptable to assume that the flume based drag coefficients calculated in Section 4.1 remained applicable in the field.

Drag forces acting on cottonwood seedlings were calculated to be as high as 156 N at a flow velocity of 1.5 m s^{-1} (Figure 9), and would be sufficient to bend all cottonwood seedlings growing on sandbars. In addition, drag forces at 1.5 m s^{-1} are likely to be capable of removing the weakest seedlings. The estimated drag force acting at this velocity (156 N) is still well below the mean values for patch resistances of cottonwood seedlings (249 and 315 N, respectively). It should, however, be noted that because these plants are elastic and not rigid, not all of the drag force applied to the stems during a flow will be transferred to the roots. At low flows this dissipation of energy by the stems will likely result in very few cottonwood seedlings being removed, and even at high flows this elastic energy loss may reduce the likelihood of all but the weakest of these plants being removed by flows, with the majority of plants simply bending over. The lines indicating drag forces in Figure 9A (one-year old seedlings) are actually slightly higher than those shown in Figure 9B (two-year old seedlings), because the drag forces measured for the lower stem density of two-year old seedlings were slightly lower than for the higher density one-year old seedlings. Additionally, by the second year of growth, rooting depth for most seedlings will have increased. Therefore, in addition to the decreased drag being applied to these seedlings, uprooting and bending resistances will increase as the plant invests more energy in above- and below-ground biomass with each additional growing season. The

probability of a SDHF removing cottonwoods from channel bars is thus reduced with each season of growth.

For reed canarygrass (Figure 10), the drag forces measured in the flume (up to 0.25 m s^{-1}) indicate that at this range of flows, the driving force acting on the grass is lower than both ranges of forces for uprooting and bending at the lower stem density of 400 stems m^{-2}. In the case of the higher stem density of 800 stems m^{-2}, higher drag forces were recorded, and under these conditions, some bending of grass stems may occur. As previously discussed for cottonwoods, grass stems are not rigid and some of the drag force is therefore absorbed by the stems and leaves of the grass, with only a portion of that force being transferred to the roots. It is therefore very unlikely that stems of this plant will be removed by flows in the range of the flume experiments. At a flow velocity of 1.5 m s^{-1}, simulating a SDHF event on the central Platte, drag forces always exceed the force required for stem bending. Some weaker or more exposed stems may experience breakage or uprooting at this flow velocity, but this is likely to be limited (the mean patch resistance for reed canarygrass was 4,560 N), and stem bending will tend to be the dominant behaviour. Note that the logarithmic scale can be somewhat misleading and that the line indicating the maximum drag force recorded for flow velocities up to 1.5 m s^{-1} for 800 stems m^{-2} represents only a very small proportion of the total range of uprooting forces for patches of reed canarygrass.

In the case of Phragmites (Figure 11), the drag forces from the flume study (up to 0.25 m s^{-1}) were lower than both the force required for bending and the force required for uprooting. At the estimated drag force for velocities up to 1.5 m s^{-1} (218 N), drag forces exceed the full range of bending forces, but are still insufficient to initiate uprooting of even the weakest and sparsest patches of Phragmites. Thus, as with reed canarygrass, bending will be the dominant behaviour at high flows.

The results presented here provide further quantitative support explanation for the findings reported in the outdoor flume experiments of Kui et al. (2014). In their experiments to investigate the location and occurrence of plant dislodgement during high discharge events, they found that only 1% of plants were removed from a sandbar during a flow event. Plants that were dislodged had shorter roots, with the probability of dislodgement only being substantial in plants whose roots were < 0.1 m in length. Further, their statistical analysis showed that for every centimeter increase in root length, the probability of dislodgement decreased by 16%.

As root length varies between and within each growing season, there is a temporal aspect to the potential for plants to be removed by flows. Of the three species studied, cottonwood seedlings are expected to show the smallest cyclical changes in above- and below-ground biomass but fine root biomass will die back in autumn and leave seedlings most susceptible to removal in winter and early

spring. This fine biomass will be renewed and the rest of the root network will be extended during the next growing season. Reed canarygrass and Phragmites are likely to show larger intra-annual changes in their above- and below-ground biomass. Indeed, Liffen et al. (2013) showed that the roots of the emergent macrophyte Sparganium erectum all but disappeared during the winter months, leaving a network of shallower rhizomes that were highly vulnerable to scour in winter and spring. In addition, the presence of annual plants such as Eragrostis, Cyperus, Xanthium and Echionochloa on the Platte (Johnson, 2000) increase the hydraulic roughness of bars and thus reduce bar top velocities and shear stresses. These points emphasize that floods timed to occur towards the beginning of the growing season have the greatest potential to remove bar top vegetation. Further, there is also a spatial sensitivity: Kui et al. (2014) found that 55% of dislodged plants were from the streamward margins of sandbars, with plants that had colonized more distal locations less likely to be removed. Nevertheless, once established, cottonwood trees, reed canarygrass and Phragmites are very resistant to removal by fluid drag because of their rooting depths and the increased complexity and interconnectivity of their rooting networks.

5.2 Quantifying potential scour around plants and effects on plant pullout

The previous section suggested that drag forces during SDHFs are insufficient to remove the three vegetation species studied here from bars, especially once vegetation has established. It is also necessary to consider how much local scour can be expected around the base of the plant stems during flows of various magnitudes and durations, and whether this local scour can affect uprooting resistance sufficiently to increase the likelihood of plant uprooting. Discharge and slope values (0.0013 m m^{-1}) were used, in combination with the normal-depth approximation, to estimate the depth of local scour around vegetation stems at three different cross sections in the Elm Creek study reach (Figure 3). Scour was predicted using three bridge-pier scour equations, over a range of flow depths up to 1.7 m, with associated discharges of up to 227 m^3s^{-1} and velocities of up to 1.5 m s^{-1}. The equations of Melville and Sutherland (1988), HEC-18 (Richardson and Davis, 2001) and Superposition of Components (Richardson and Davis, 2001)were used to compare possible ranges of equilibrium scour depths, taking into account the different mean stem diameters for each species as measured in the field.

Results showed that equilibrium scour depths could range from 5 to 55 mm around Phragmites stems and 5 to 35 mm around reed canarygrass stems and cottonwood seedlings at the three sites. Predicted values of local scour depths around stems of bar top vegetation were thus shown to be relatively small compared to the rooting depths of the plants measured in the field, in particular Phragmites. The results from the analysis presented here suggest that equilibrium (maximum) scour depths, even at very high discharges would be insufficient to scour all but the shallowest rooted vegetation.

Furthermore, as the equilibrium (maximum) scour depth equations were developed for rigid bridge piers rather than flexible plant stems, the predicted values provide upper estimates of scour depths. Newly germinated cottonwood seedlings and other annual species could, however, be scoured at high flows where rooting depths have not yet greatly exceeded the potential scour depths of up to 55 mm at 227 $m^3 s^{-1}$ and up to 67 mm at the 100-year recurrence interval of approximately 782 $m^3 s^{-1}$ at the gauge at Overton. Similar to the discussion in the section on drag forces, the implication of these results is that the timing of any SDHFs proposed by PRRIP should take into account the onset of the growing season, and potential time for root growth between SDHF events. The scour results also suggest that once bar vegetation has established, and rooting depths have exceeded potential local scour depths, even at high flows during the 100-year recurrence interval, the combination of drag and scour are unlikely to remove the three species tested in this study. The magnitude of flow, therefore, required to remove established bar vegetation through drag and vertical local scour of bars in the central Platte River would have a recurrence interval greater than the 100-year event. Another process that could expose roots would be the migration of bedform features. Although bedforms were not studied in detail as part of this study, an initial analysis suggests that at 227 $m^3 s^{-1}$ a flow depth of about 0.4 m over the bar tops could be expected. At this flow depth, and assuming a dune height approximately 0.3 times the flow depth, the biggest dunes are estimated to be about 0.12 m. At the 100-year recurrence interval flow depth over the bars is predicted to be approximately 0.95 m with an expected dune height of approximately 0.29 m. However, the presence of vegetation would likely interrupt the flow structures that drive both ripple and dune formation, so this process of bedform migration is likely of little significance to the exposing of roots and subsequent vegetation removal from bars.

Further to this analysis of scour are the effects of plant patches on local deposition. Yong and Nepf (2010) and Ortiz et al. (2013) showed for example, that deposition was likely to occur downstream of rigid emergent vegetation because mean and turbulent velocities are reduced in this region. In contrast, however, deposition was not seen downstream of patches of flexible submerged vegetation because of the way these plants changed the flow structure surrounding them. Ortiz et al. (2013) also recognized that the morphological feedbacks between the plants and their substrate differed between rigid and flexible vegetation, with positive feedback and patch expansion likely to occur downstream of rigid emergent vegetation, such as Phragmites in the Platte River, and negative feedback and inhibition of patch growth in stands of flexible submergent vegetation, such as young cottonwood seedlings.

5.3 Spatial analysis of flow velocities capable of uprooting plants through drag forces

To better understand the real-world significance of the experimental and modelling results presented in this study, an attempt has been made to determine the spatial patterns of flow velocities capable of uprooting patches of each plant species studied. PRRIP provided the authors with SRH-2D model (Lai, 2008; 2010; 2011; Lai and Greimann, 2008; 2010; Lai et al., 2011) output for a flow event of 227 m^3s^{-1}. The velocity required to initiate plant uprooting (minimum patch resistances modelled in RipRoot runs) and to remove all plants of that species (maximum patch resistance modelled in RipRoot runs) were calculated by taking the minimum and maximum forces in Figures 9-11 and solving for velocity. Maps were then created to indicate the likelihood of plant uprooting within the Elm Creek reach. Flow velocities that are too low to remove any plants are shown in dark green. Locations where velocities are sufficient to initiate the uprooting of the weakest plants are indicated in light green. The colour scale then transitions through yellow to orange, indicating higher flow velocities and zones where a greater percentage of the plants might be expected to be uprooted during a 227 m^3s^{-1} flow. Areas shaded red indicate parts of the channel where velocities are high enough to uproot all plants of that species. Finally, the isovels were overlain by the locations of bars in 2010 (also provided by PRRIP) so that velocities on and around bars where vegetation is a management concern can be isolated from the channels.

There is only one location in the study reach where no uprooting of one-year old cottonwoods is predicted during a 227 m^3s^{-1} flow (dark green; area has a higher elevation) (Figure 12A). Only the weakest cottonwood seedlings should be uprooted (mid-green) at the majority of channel margins. The velocities over bar areas mostly suggest the potential for flow to uproot a higher proportion of one-year old cottonwood seedlings than at channel margins (light green), but the deepest rooted, strongest seedlings will be difficult to remove from most bar locations through drag forces alone (indicated by an absence of yellow to red zones overlaying bar regions). The exact percentage of plants removed would be site specific and would vary, for example, according to plant areal density, typical water table depths and resulting rooting depths. Overall, the map suggests that partial removal of the weakest and most exposed one-year old cottonwood seedlings is likely on vegetated bars in the Elm Creek reach during a 227 m^3s^{-1} flow event. In general, flow velocities over the bars were higher downstream of the Kearney Canal (a diversion that provides irrigation water and power during irrigation season through a 16 mile long canal extending from southwest of Elm Creek, Nebraska to the town of Kearney, Nebraska), as indicated by the presence of greater proportions of light green compared to mid-green upstream of the diversion. As such, more one-year old cottonwoods could be expected to be removed downstream compared to upstream of the diversion.

The map showing uprooting velocities for two-year old cottonwood seedlings (Figure 12B) shows similar results to the map for one-year old cottonwood seedlings: the flow velocities over the bar areas during and 227 m^3s^{-1} flow event are sufficient to uproot the weakest and/or most exposed seedlings (areas indicated in mid to light green). For two-year old cottonwoods, velocities capable of removing all plants, as predicted by RipRoot patch modelling, do not exist anywhere in this reach at 227 m^3s^{-1}, even around the diversion.

The distribution of flow velocities capable of uprooting patches of reed canarygrass are shown in Figure 13. Almost all parts of the channel are shaded in dark green, indicating that velocities are too low to remove even the weakest patches of grass in these locations. Areas of mid-green (indicating initiation of uprooting of the weakest stems) can be seen in some parts of the reach, but these correspond to deeper parts of the channel, rather than bars. Removal of reed canarygrass through drag forces alone is therefore very unlikely once this species has established on bars, both upstream and downstream of the diversion. When it is also considered that bending will occur before uprooting occurs, the likelihood of uprooting of this species once established is further decreased.

The map of flow velocities capable of uprooting Phragmites stems in the Elm Creek reach (Figure 14) shows that there are no locations where uprooting is likely to occur through drag forces alone, even during a 227 m^3s^{-1} flow event. It should be noted that the threshold velocity for uprooting of this species to start is ~10.6 m s^{-1} which is far beyond the velocities experienced within this reach. Once established therefore, for removal of this species to occur either other fluvial processes must also be at work, for example lateral scour and undercutting at bar edges or ice scour or human intervention must take place. The process of lateral erosion at bank and bar edges is a particularly important process, and the subject of a follow up study (Bankhead and Simon, in review), along the same study reach. The results of modelling to quantify potential lateral erosion rates under various vegetation types and densities along this reach emphasizes the importance of the depth of the root zone relative to bar height and flow elevations. The extensive root and rhizome networks of reed canarygrass and Phragmites provides greater protection to the bar material than the roots of cottonwood seedlings, but modelling showed that once root zones of reed canarygrass and Phragmites had been undermined, the width of the failure blocks could exceed those of failures involving cottonwood seedlings. The dynamics of this process, and resulting impacts on vegetation proliferation and channel planform are discussed further in Bankhead and Simon (in review).

Inundation of the bar vegetation is another mechanism that could also lead to plant mortality. For example, Auchincloss et al. (2012) showed that inundation periods of greater than 14 days significantly increases cottonwood seedling mortality to >50% of the seedling population. However, reed canarygrass and Phragmites can survive prolonged flooding (Apfelbaum and Sams, 1987) due to the presence of anoxia-tolerant rhizomes (Brandle, 1983). Cottonwood seedlings are therefore more

likely to be affected by mortality due to inundation, leaving reed canarygrass and Phragmites again as the largest problem for plant management. Management techniques such as spraying and disking are probably necessary to remove established stands of Phragmites, but SDHF events may then be able to maintain vegetation free bars once mature vegetation is cleared.

5.3.1 Comparison of predicted plant removal with field observations

Figures 12-14 suggest certain patterns and locations of velocities capable of uprooting each studied plant species through drag forces alone. In this section these patterns, and other findings during fieldwork are compared to monitoring data collected as part of the 2012 Annual Monitoring Report conducted by PRRIP for the Elm Creek reach, to assess whether the findings of this study accurately represent what is happening in the reach.

The 2012 monitoring report stated that the average height of green lines (lowest lines of perennial vegetation above baseflow elevation) were similar between the May and Aug/September surveys, with, "a slight, but statistically insignificant increase in the upstream part of the reach, and a somewhat larger (1.7 feet [0.52 m] in May to 1.8 feet [0.55 m] in Aug/Sept), but still statistically insignificant increase in the downstream part of the reach" (Tetra Tech, 2012). This finding confirms the suggestion made in the previous section, that more vegetation removal is likely downstream of the Kearney Canal Diversion than upstream (green line increased more downstream than upstream). The differences seen above and below the diversion are in part a result of higher flow velocities, but other factors such as plant submergence may also affect survival rates. The monitoring report also notes that some bars had experienced significant erosion, indicating that processes other than drag forces, also play a role in determining plant survival on bars.

Another interesting finding of the 2012 monitoring report was that although disking in Fall 2010 had been successful in breaking up the Phragmites root mat, rhizome fragments still present in the bars were able to regenerate and form dense stands the following growing season. The field notes collected as part of this study also suggested that rhizomes of sprayed areas looked healthy, even where the above ground biomass was dead and brittle. As Phragmites can regenerate in the growing season following disking and/or spraying and velocities are insufficient to uproot this plant even during SDHFs, the continued need for management through disking and spraying seems likely.

Comparison of frequency of occurrence of each species between the May and August/September 2011 surveys, with the results suggested by the maps in Figures 12-14, showed generally similar trends. For example, the monitoring report found that there was a decline in cottonwood frequency in some areas (the elevations corresponding to discharges of 34.0 to 85.0 m^3s^{-1}) between the May and August/September surveys, suggesting that flows during this period created velocities high enough to remove the weaker seedlings of this species. The most commonly occurring species during the

August/September survey in all elevation ranges were Phragmites and cottonwood, confirming that: 1) Phragmites is very difficult to remove through drag forces; and 2) even though the weaker cottonwood seedlings can be removed, a large proportion of seedlings remained on the bars even after high flows. The report also notes a substantial cover of reed canarygrass in the 85.0 to 142 m^3s^{-1} range, again confirming that once established this species is difficult to remove even during SDHFs. The map in Figure 13 suggests that no removal of reed canarygrass is likely at any bar elevations during a 227 m^3s^{-1} SDHF, so decreased prevalence of this species below 85.0 m^3s^{-1} elevations may be a result of other processes. As both reed canarygrass and Phragmites are tolerant to long period of inundation, scour of these plants at bar edges seems to be the most likely removal process.

6 CONCLUSIONS

The present study combined several approaches to try to determine whether floods of up to 227 m^3s^{-1} through the central Platte River would be capable of removing cottonwood, Phragmites and reed canarygrass stands of various ages and densities from mid-channel and lateral bars.

A comparison of drag (driving) forces measured in a flume study, with uprooting (resisting) forces measured in the field showed that limited numbers of cottonwood seedlings may be removed by drag forces alone at high flows, but that stem bending will dominate uprooting for reed canarygrass and Phragmites. For cottonwoods, the likelihood of seedling removal will decrease with each additional year of growth, as rooting depths increase and reduced stem density reduces drag forces acting on a stand of seedlings. Established cottonwood trees, reed canarygrass, and Phragmites are very resistant to removal through drag forces applied by high flows. Johnson (1997) also noted that once vegetation establishes, the roots of the most common Platte River riparian species grow sufficiently that they stabilize their substrate and resist erosion.

In this study, predicted values of local scour around stems of bar vegetation were shown to be relatively small compared to the rooting depths of the plants measured in the field, in particular Phragmites. The results presented here suggest that even at very high discharges, equilibrium (maximum) scour depths, would be insufficient to scour all but the shallowest rooted vegetation. Newly germinated cottonwood seedlings and other annual species may be scoured at high flows where rooting depths have not yet greatly exceeded the potential scour depths of up to 55 mm at 227 m^3s^{-1} and up to 67 mm at the 100-year recurrence interval of approximately 782 m^3s^{-1}. These results confirm the idea that once bar top vegetation has established, and rooting depths have exceeded potential local scour depths, the combination of drag and scour are unlikely to remove the three species tested in this study. Another possible removal mechanism that was not studied here, is the

potential removal of vegetation from bar and bank edges through the interconnected processes of hydraulic erosion and geotechnical failure.

The study presented here shows the importance of vegetation as an ecosystem engineer, with both above- and below-ground biomass interacting to develop the feedbacks between vegetation and channel planform. This research has highlighted in particular, the impact of exotic invasive species on the predicted performance of in-stream flow management actions. The proposed magnitude of the SDHFs investigated here was developed prior to the proliferation of Phragmites and reed canarygrass in the central Platte River. These species appear to be much more resistant to scour than the native species (cottonwood and willow) that are responsible for historical episodes of channel narrowing. PRRIP stakeholders have attempted to adjust to these invading species by teaming with other stakeholders to implement a massive Phragmites control effort. However, it is becoming apparent that some level of ongoing mechanical control will be necessary to control this species.

7 ACKNOWLEDGEGMENTS

This research was funded by the Platte Recovery and Restoration Implementation Program (PRRIP). The authors wish to acknowledge the efforts of Carrie Hinners and Jiana Stovers for field assistance, Lee Patterson for construction of novel field apparatus and field assistance, Ibrahim Tabança for field and laboratory assistance and Danny Klimetz for map preparation. Flume experiments were designed, set up and run with the assistance of Gareth M. Keevil.

8 REFERENCES

Aberle, J. and Järvelä, J.2013. Flow resistance of emergent rigid and flexible vegetation. Journal of Hydraulic Research, 51(1). DOI: 10.1080/00221686.2012.754795.

Abernethy, B., and Rutherfurd, I.D. 2001. The distribution and strength of riparian tree roots in relation to riverbank reinforcement. Hydrological Processes, 15: 63-79.

Apfelbaum, S.I. and C.E. Sams. 1987. Ecology and control of reed canary grass (Phalaris arundinacea L.). Natural Areas Journal 7(2): 69-74.

Auchincloss, L.C., J.H. Richards1, Young, C.A., and Tansey, M.K. 2012. Inundation Depth, Duration, and Temperature Influence Fremont Cottonwood (Populus fremontii) Seedling Growth and Survival. Western North American Naturalist 72(3):323-333. 2012. doi: http://dx.doi.org/10.3398/064.072.0306

Bennett, S.J., Bridge, J.S., and Best, J.L. 1998. The fluid and sediment dynamics of upper-stage plane beds. Journal of Geophysical Research 103: 1239-1274.

Bennett, S.J., Pirim, T., and Barkdoll, B.D. 2002. Using simulated emergent vegetation to alter stream flow direction within a straight experimental channel. Geomorphology, 44: 115-126.

Bertram, H.-U., 1984. Uber die hydraulische Berechnung von Gerinnen mit Uferbewuchs. Zeitschrift für Kulturtechnik und Flurbereinigung, 25: 77-86.

Brändle R. (1983): Evolution der Gärungskapazität in den flut- und anoxiatoleranten Rhizomen vonPhalaris arundinacea, Phragmites communis, Schoenoplectus lacustris undTypha latifolia.Bot. Helv. 93: 39–45.

Coppin, N.J., and Richards, I.G. 1990. Use of Vegetation in Civil Engineering. Butterworths, London, UK.

Daniels, H.E. 1945. The statistical theory of the strength of bundles of threads. I. Proceedings of the Royal Society of London, Series A, 183(995): 405-435.

Danjon, F., Barker, D.H., Drexhage, M., and Stokes, A. 2008. Using three-dimensional plant root architecture in models of shallow-slope stability. Annals of Botany, 101(8): 1281-1293.

De Baets, S., Poesen, J., Reubens, B., Wemans, K., De Baerdemaeker, J., and Muys, B. 2008. Root tensile strength and root distribution of typical Mediterranean plant species and their contribution to soil shear strength. Plant and Soil, 305: 207-226.

Docker, B.B., and Hubble, T.C.T. 2008. Quantifying root-reinforcement of river bank soils by four Australian tree species. Geomorphology, 100: 401-418.

Dunn, C., López, F., and García, M.H. 1996. Mean flow and turbulence structure induced by vegetation: Experiments. Hydraulic Engineering Series No. 50, UILU-ENG 96-2009, Department of Civil Engineering, University of Illinois at Urbana-Champaign, Urbana, IL.

Edmaier, K., P. Burlando, and P. Perona (2011), Mechanisms of vegetation uprooting by flow in alluvial non-cohesive sediment, Hydrology and Earth System Sciences, 15(5), 1615-1627, doi: 10.5194/hess-15-1615-2011.

Ennos, A.R. 1990. The Anchorage of leek Seedlings: The Effect of Root Length and Soil Strength. Annals of Botany, 65: 409-416.

Fan, C.-C., and Su, C.-F. 2008. Role of roots in the shear strength of root-reinforced soils with high moisture content. Ecological Engineering, 33(2): 157-166.

Fathi-Moghadam, M., and Kouwen, N. 1997. Nonrigid, nonsubmerged, vegetative roughness on floodplains. Journal of Hydraulic Engineering, ASCE, 123(1): 51-57.

Fredlund, D.G., Morgenstern, N.R., and Widger, R.A. 1978. The shear strength of unsaturated soils. Canadian Geotechnical Journal, 15(3): 313-321.

Freeman, G.E., Rahmeyer, W.H., and Copeland, R.R. 2000. Determination of resistance due to shrubs and woody vegetation. USACE Report ERDC/CHL TR-00-25. USACE ERDC, Vicksburg.

Friedkin, J.F. 1945. A Laboratory Study of the Meandering of Alluvial Rivers. US Waterways Experiment Station, Vicksburg.

Genet, M., Stokes, A., Salin, F., Mickovski, S.B., Fourcaud, T., Dumail, J., and van Beek, R. 2006. The influence of cellulose content on tensile strength in tree roots. Plant and Soil, 278: 1-9.

Gray, D.H., and Sotir, R.B. 1996. Biotechnical and Soil Bioengineering Slope Stabilization: A Practical Guide for Erosion Control. John Wiley & Sons, Inc., New York, NY.

Greenway, D.R. 1987. Vegetation and slope stability. In: M.G. Anderson and K.S. Richards, eds. Slope Stability. John Wiley & Sons Ltd., Chichester, UK: 187-230.

Hadley, R.F., Karlinger, M.R., Burns, A.W., and Eschner, T.R. 1987. Water development and associated hydrologic changes in the Platte River, Nebraska, U.S.A. Regulated Rivers: Research and Management, 1: 331-341.

Hales, T.C., Ford, C.R., Hwang, T., Vose, J.M., and Band, L.E. 2009. Topographic and ecologic controls on root reinforcement. Journal of Geophysical Research, 114, F03013, doi:10.1029/2008JF001168.

Hidalgo, R.C., Kun, F., and Herrmann, H.J. 2001. Bursts in a fiber bundle model with continuous damage. Physical Review E, 64(6), 066122, doi:10.1103/PhysRevE.64.066122.

Hopkinson L, Wynn T. 2009. Vegetation impacts on near bank flow. Ecohydrology, online, pp. 1–15.

James, C.S., Goldbeck, U.K., Patini, A., and Jordanova, A.A. 2008. Influence of foliage on flow resistance of emergent vegetation. Journal of Hydraulic Research, 46(4): 536-542. doi:10.3826/jhr.2008.3177.

Järvelä, J. 2002. Flow resistance of flexible and stiff vegetation: a flume study with natural plants. Journal of Hydrology, 269(1-2): 44-54.

Järvelä, J. 2004. Determination of flow resistance caused by non-submerged woody vegetation. International Journal of River Basin Management, 2(1): 61-70.

Johnson, W.C. 1994. Woodland Expansions in the Platte River, Nebraska: Patterns and Causes. Ecological Monographs, 64 (1): 45-84.

Johnson, W. C. 1997. Equilibrium response of riparian vegetation to flow regulation in the Platte river, Nebraska. Regulated Rivers: Research & Management, 13: 403–415. doi: 10.1002/(SICI)1099-1646(199709/10)13:5<403::AID-RRR465>3.0.CO;2-U

Johnson, W.C. 2000. Tree recruitment and survival rates in rivers: influence of hydrological processes. Hydrological Processes, 14(16-17): 3051-3074.

Kui, L., Stella, J,, Lightbody. A., Wilcox, A.C. 2014. Ecogeomorphic feedbacks and flood loss of riparian tree seedlings in meandering channel experiments. Water Resources Research, 50(12), doi: 10.1002/2014WR015719

Lane, E.W. 1957. A study of the shape of channels formed by natural streams flowing in erodible material. Missouri River Division Sediment Series 9. U.S. Army Engineer Division, Missouri River, Omaha, NE.

Leopold, L.B. and Wolman, M.G. 1957. River channel patterns: braided, meandering and straight. U.S. Geological Survey Professional Paper 282-B. U.S. Government Printing Office, Washington, D.C.

Li, R.-M., and Shen, H.W. 1973. Effect of tall vegetations on flow and sediment. Journal of the Hydraulics Division, ASCE, 99(HY5): 793-814.

Liffen, T., Gurnell, A., O'Hare, M.T. 2013. Profiling the below ground biomass of an emergent macrophyte using an adapted ingrowth core method. Aquatic Botany, 110:97-102.

Liffen, T., Gurnell, A., O'Hare, M., Pollen-Bankhead, N., and Simon, A. 2011. Biomechanical properties of the emergent aquatic macrophyte Sparganium erectum: implications for landform development in low energy rivers. Ecological Engineerin, 37(11),1925-1931

Loades, K.W., Bengough, A.G., Bransby, M.F., and Hallett, P.D. 2009. Planting density influence on fibrous root reinforcement of soils. Ecological Engineering, 36(3): 276-284.

López, F., and García, M.H. 2001. Mean flow and turbulence structure of open-channel flow through non-emergent vegetation. Journal of Hydraulic Engineering, ASCE, 127(5): 392-402.

McBride, M., Hession, W.C., Rizzo, D.M., and Thompson, D.M. 2007. The influence of riparian vegetation on near-bank turbulence: a flume experiment. Earth Surface Processes and Landforms, 32(13): 2019-2037.

Melville, B.W., and Sutherland, A.J., 1988, Design method for local scour at bridge piers:American Society of Civil Engineering, Journal of the Hydraulics Division, v. 114, no. 10,p. 1210–1225.

Mickovski, S.B., Hallet, P.D., Bransby, M. F., Davies, M.C.R., Sonnenberg, R., and Bengough, A.G. 2009. Mechanical Reinforcement of Soil by Willow Roots: Impacts of Root Properties and Root Failure Mechanism. Soil Science Society of America Journal, 73: 1276-1285.

Möller I, Spencer T, French JR, Leggett DJ, Dixon M. 1999. Wave transformation over salt marshes: a field and numerical modelling study from North Norfolk, England. Estuarine, Coastal and Shelf Science 49: 411–426.

Mosley, M.P. 2001. Discussion of Paola, C. Modelling stream braiding over a range of scales. In: M.P. Mosley, ed. Gravel-Bed Rivers V. New Zealand Hydrological Society, Wellington: 11-46.

Murphy et al., 2004 P.J. Murphy, T.J. Randle, L.M. Fotherby and J.A. Daraio, The Platte River Channel: History and Restoration, U.S. Dept. of Int., Bur. of Reclamation report, Denver, CO (2004) 167 pp.Nanson, G.C., and Knighton, A.D. 1996. Anabranching rivers: their cause, character and classification. Earth Surface Processes and Landforms, 21: 217-239.

Nepf, H.M. 1999. Drag, turbulence, and diffusion in flow through emergent vegetation. Water Resources Research, 35(2): 479-489.

Ortiz, A. C., Ashton, A., and H. Nepf. 2013. Mean and turbulent velocity fields near rigid and flexible plants and the implications for deposition, Journal of Geophysical Research: Earth Surface, 118(4), 2585-2599, doi: 10.1002/2013jf002858.

Paola, C. 2001. Modelling stream braiding over a range of scales. In: M.P. Mosley, ed. Gravel-Bed Rivers V. New Zealand Hydrological Society, Wellington: 11-46.

Pasche, E., and Rouvé, G. 1985. Overbank flow with vegetatively roughened flood plains. Journal of Hydraulic Engineering, ASCE, 111(9): 1262-1278.

Paul, M., Thomas, R.E., Dijkstra, J.T., Penning, W.E. and Vousdoukas, M.I. 2013. Plants, hydraulics and sediment dynamics. In. Users guide to ecohydraulic modelling and experimentation. Ed. Peter A. Davies, pp 91-116.

Petryk, S., and Bosmajian, G. 1975. Analysis of flow through vegetation. Journal of the Hydraulics Division, ASCE, 101(HY7): 871-884.

Pollen, N. 2007. Temporal and spatial variability in root-reinforcement of streambanks: Accounting for soil shear strength and moisture. Catena, 69: 197-205.

Pollen, N., and Simon, A. 2005. Estimating the mechanical effects of riparian vegetation on streambank stability using a fiber bundle model. Water Resources Research, 41: W07025, doi:10.1029/2004WR003801.

Pollen-Bankhead, N., Thomas, R.E., Gurnell, A., Liffen, T., and Simon. 2011. Quantifying the potential for flow to remove the emergent macrophyte Sparganium erectum from the margins of low energy rivers. Ecological Engineering, 37(11),1779-1788

Pollen-Bankhead, N., and Simon, A. 2009. Enhanced application of root-reinforcement algorithms for bank-stability modeling. Earth Surface Processes and Landforms, 34(4): 471-480.

Pollen, N., Simon, A., and Collision, A.J.C. 2004. Advances in Assessing the Mechanical and Hydrologic Effects of Riparian Vegetation on Streambank Stability. In: S.J. Bennett and A. Simon, eds. Riparian Vegetation and Fluvial Geomorphology, Water Science and Applications 8, AGU, Washington, D.C.: 125-139.

Pollen-Bankhead, N., Simon, A., and Thomas, R. 2013. The reinforcement of soil by roots: recent advances and directions for future research. In: Hupp, C.R. (ed.), Treatise in Geomorphology. Elsevier. New York.

Potyondy, J.G., 1961. Skin friction between various soils and construction materials. Geotechnique, 11(4): 339-353.

Richardson, E.V., and Davis, S.R. 2001. Evaluating Scour at Bridges, Fourth Edition. Hydraulic Engineering Circular 18, Publication Number FHWA NHI 01-001. Federal Highway Administration, U.S. Department of Transportation, Washington, D.C.

Riestenberg, M., and Sovonick-Dunford, S.S. 1983. The role of woody vegetation in stabilizing slopes in the Cincinnati area, Ohio. Geological Society of America Bulletin, 94(4): 506-518.

Schnauder, I., and Wilson, C.A.M.E. 2009. Discussions. Journal of Hydraulic Research, 47(3): 384-386. DOI: 10.1080/00221686.2009.9522010.

Schwarz, M., Preti, F., Giadrossich, F., Lehmann, F., and Or, D. 2010. Quantifying the role of vegetation in slope stability: A case study in Tuscany (Italy). Ecological Engineering, 36(3): 285-291.

Simon, A., and Collison, A.J.C. 2002. Quantifying the mechanical and hydrologic effects of riparian vegetation on streambank stability. Earth Surface Processes and Landforms, 27(5): 527-546.

Simon, A., Pollen-Bankhead, N. and Thomas, R.E., 2011. Iterative Bank-Stability and Toe-Erosion Modeling for Stream Restoration Design. In: Simon, A., S.J. Bennett, J. Castro and C.R. Thorne (eds.), Stream Restoration in Dynamic Systems: Scientific Approaches, Analyses, and Tools. American Geophysical Union: Washington.

Simon, A., Pollen, N., and Langendoen, E.J. 2006. Influence of Two Woody Riparian Species on Critical Conditions for Streambank Stability: Upper Truckee River, California. Journal of the American Water Resources Association, 42(1): 99-**113.**

Simpson, C.J., and Smith, D.G. 2001. The braided Milk River, northern Montana, fails the Leopold-Wolman discharge-gradient test. Geomorphology, 41: 337-353.

Smith, N.D. 1970. The braided stream depositional environment: comparison of the Platte River with some Silurian clastic rocks, North-Central Appalachians. Geological Society of America Bulletin, 81(10): 2993-3014.

Smith, D.G., and Smith, N.D. 1980. Sedimentation in anastomosed river systems: examples from alluvial valleys near Banff, Alberta. Journal of Sedimentary Petrology, 50(1): 157-164.

Stone, B.M., and Shen, H.T. 2002. Hydraulic resistance of flow in channels with cylindrical roughness. Journal of Hydraulic Engineering, ASCE, 128(5): 500-506.

Tanino, Y. and H. M. Nepf. 2008. Lateral dispersion in a random cylinder array at high reynolds number. J. Fluid Mech. 600, 339- 371.

Terzaghi, K., and Peck, R.B. 1967. Soil Mechanics in Engineering Practice (2nd Edition). John Wiley & Sons, Inc., New York, NY.

Thomas, R.E., and Pollen-Bankhead, N. 2010. Modeling root-reinforcement with a fiber-bundle model and Monte Carlo simulation. Ecological Engineering, 36(1): 47-61.

Thorne, C.R., and Abt, S.R. 1993. Analysis of riverbank instability due to toe scour and lateral erosion. Earth Surface Processes and Landforms, 18: 835-843.

Tosi, M. 2007. Root tensile strength relationships and their slope stability implications of three shrub species in the Northern Apennines (Italy). Geomorphology, 87: 268-283.

Waldron, L.J., and Dakessian, S. 1981. Soil reinforcement by roots: Calculation of increased soil shear resistance from root properties. Soil Science, 132(6): 427-435.

White, B.L., and Nepf, H.M. 2008. A vortex-based model of velocity and shear stress in a partially vegetated shallow channel. Water Resources Research, 44(1): W01412. doi:10.1029/2006WR005651.

Wilson, C.A.M.E., Stoesser, T., Bates, P.D., and Batemann Pinzen, A. 2003. Open channel flow through different forms of submerged flexible vegetation. Journal of Hydraulic Engineering, ASCE, 29(11): 847-853.

Wilson, C.A.M.E., Yagci, O., Rauch, H.-P., and Stoesser, T. 2006. Application of the drag force approach to model the flow-interaction of natural vegetation. International Journal of River Basin Management, 4(2): 137-146.

Wu, T.H., McKinnell III, W.P., and Swanston, D.N. 1979. Strength of tree roots and landslides on Prince of Wales Island. Alaska. Canadian Geotechnical Journal, 16: 19-33.

Zong, L. and Nepf, H. 2010. Flow and deposition in and around a finite patch of vegetation. Geomorphology, 116(3-4): 363-372.

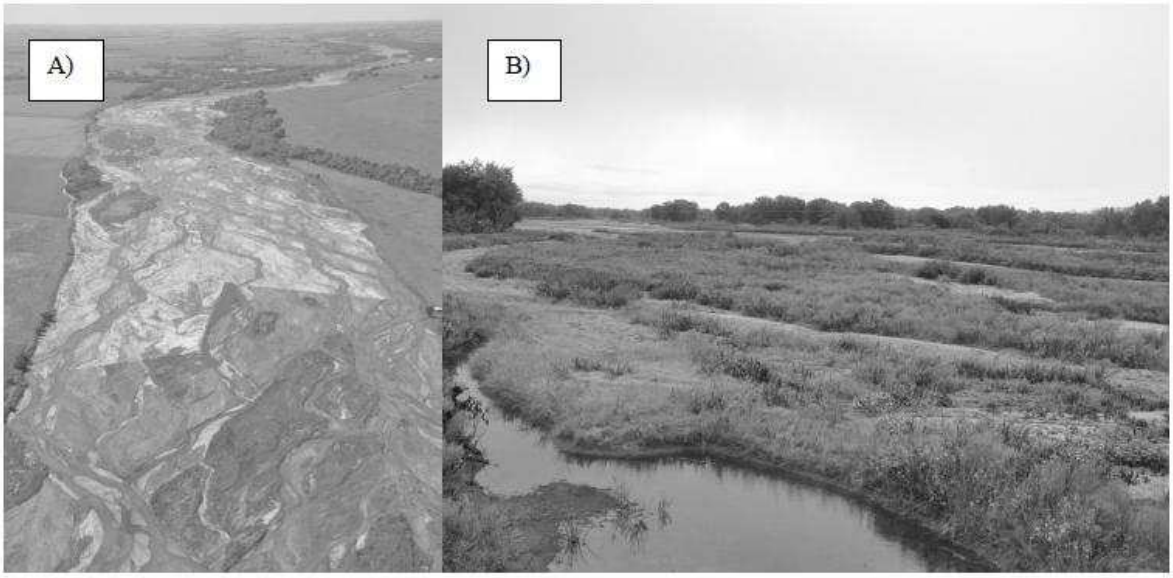

Figure 1. A) Low-level aerial view of the Platte River in an area that has been partially cleared of vegetation B) In-channel view of a vegetated part of the Central Platte River Images courtesy of Platte River Recovery Implementation Program.

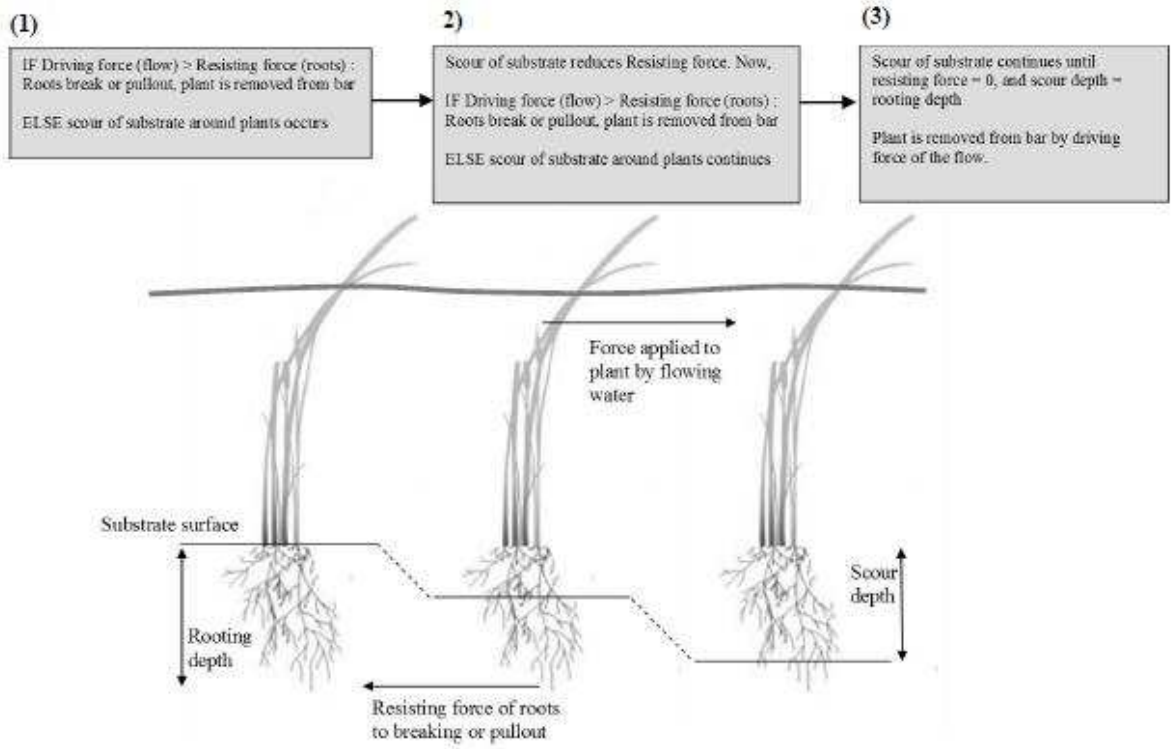

Figure 2. Continuum of processes for plant removal showing possible scenarios for balance of driving forces (flow) and resisting forces (roots). At the left end of the figure (1), driving force exceeds root strength and the plant can be removed without scour of the substrate. At the right end of the figure (3), scour has reduced the resisting force of the roots to zero, and the plant is removed by the force of the flow. In reality plant removal is likely to occur at some point between (1) and (3) at a point (2) along the continuum where scour has reduced the resisting force of the roots to a point where the flow can remove the plant from its substrate.

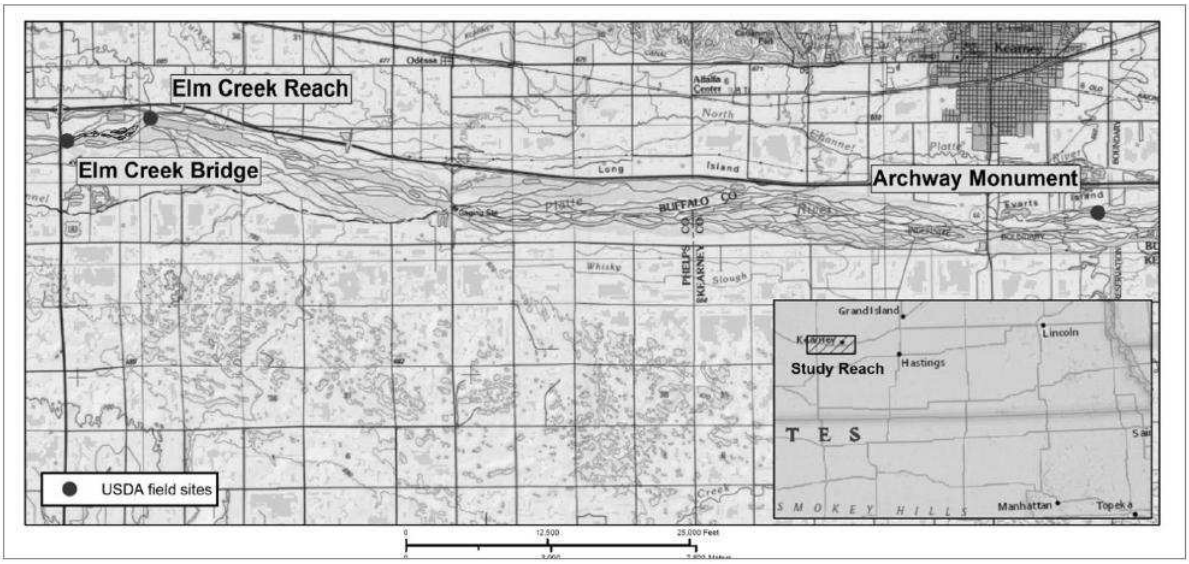

Figure 3. Map showing the location of the three vegetation study sites in this study.

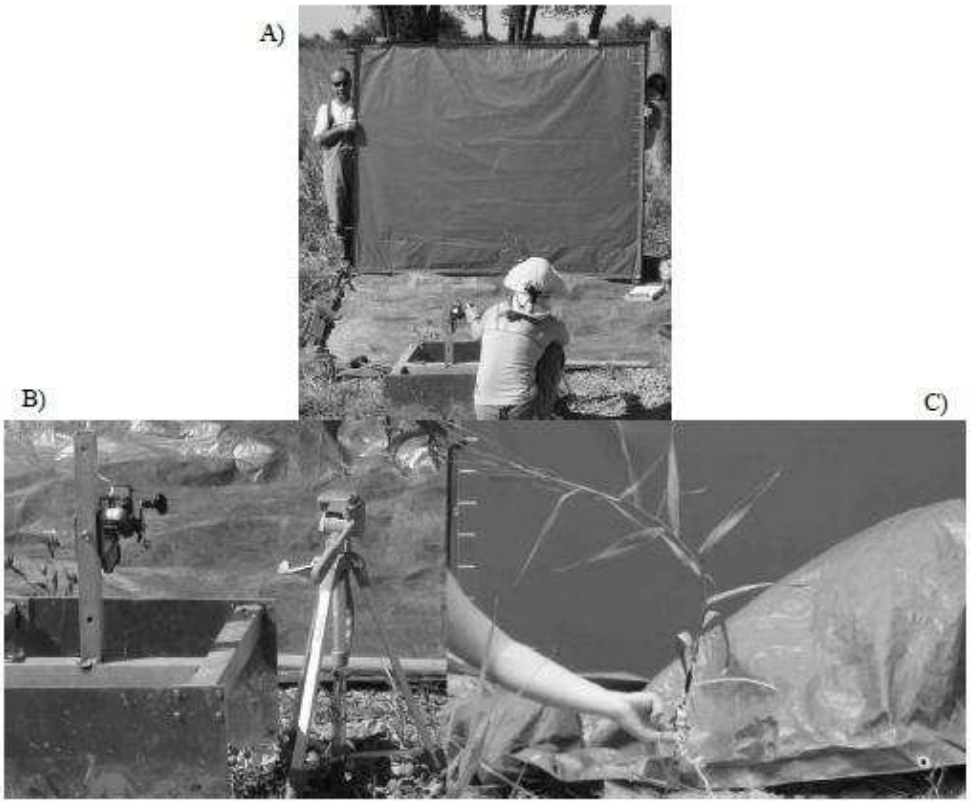

Figure 4. A) Plant bending apparatus showing reel, telescopic arm, specially-designed mount and camera tripod. B) Close up of load cell during bending test. C) View of the bending test apparatus in action.

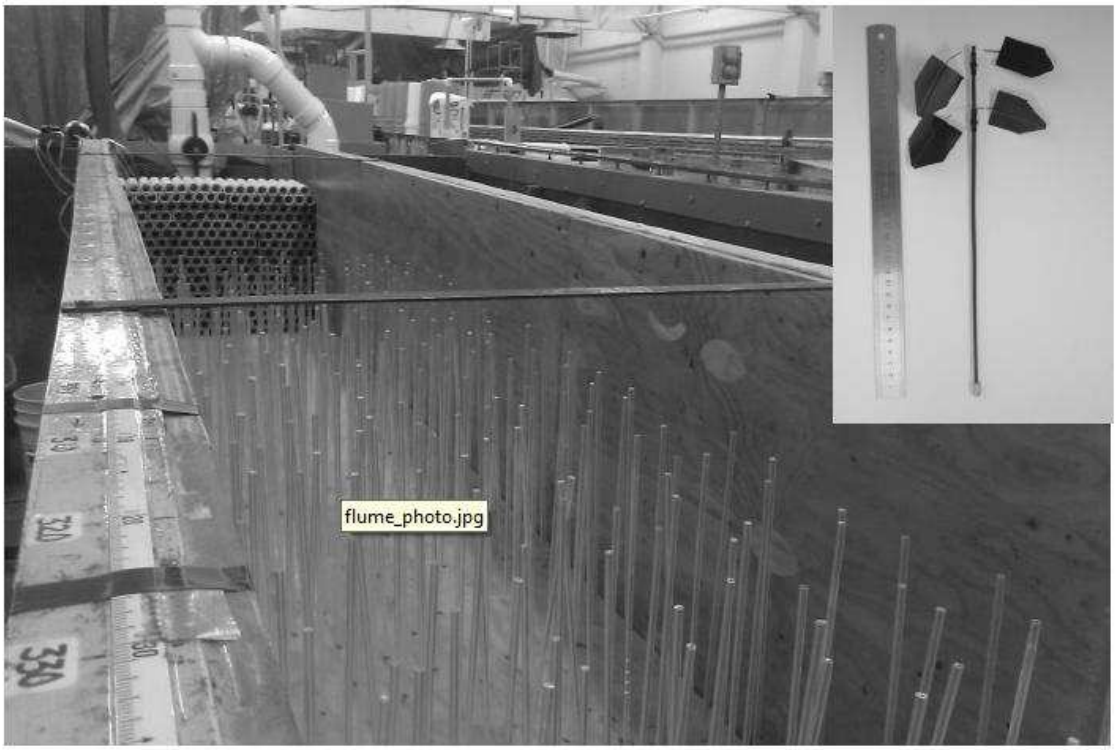

Figure 5. Example of the flume set up for a *Phragmites* run, and inset picture showing modified dowels for cottonwood plant runs, with addition of synthetic leaves.

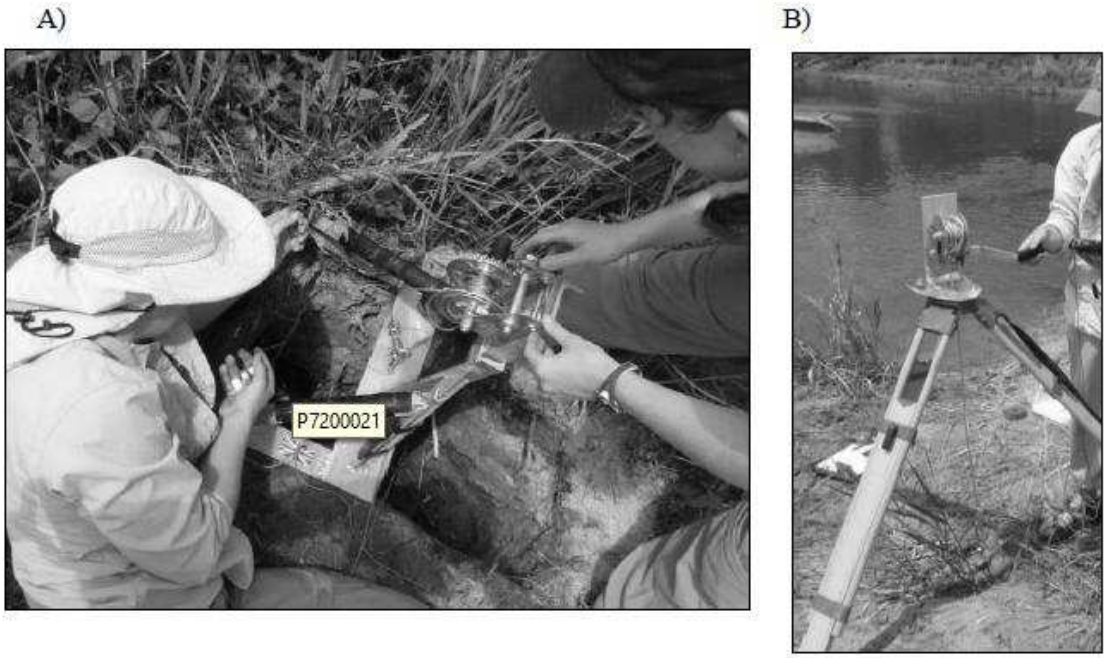

Figure 6. A) Root pulling device used to measure breaking forces of roots and rhizomes and B) Plant-pulling device being used to measure the force required to extract young *Phragmites* stems from a sandbar in the Elm Creek reach along the Platte River, NE.

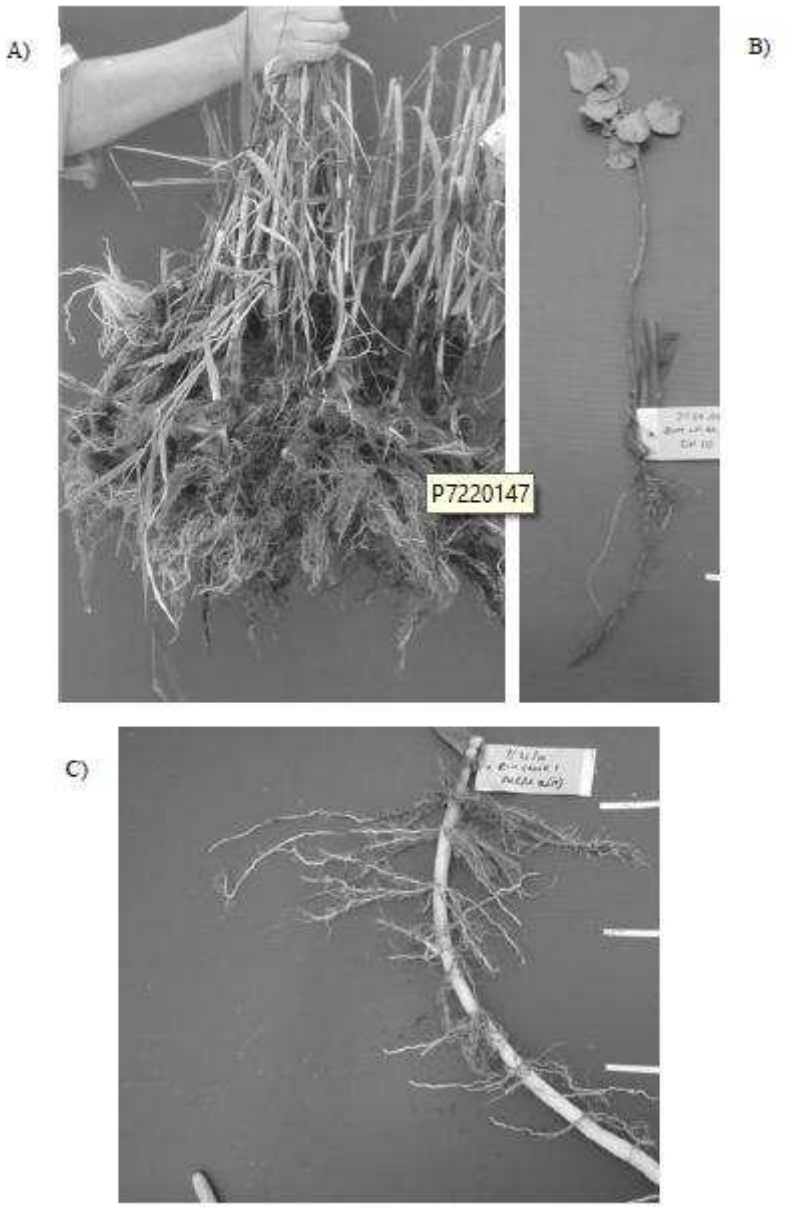

Figure 7. A) Rootball of reed canarygrass B) 1-year-old cottonwood seedling and C) a *Phragmites* rhizome

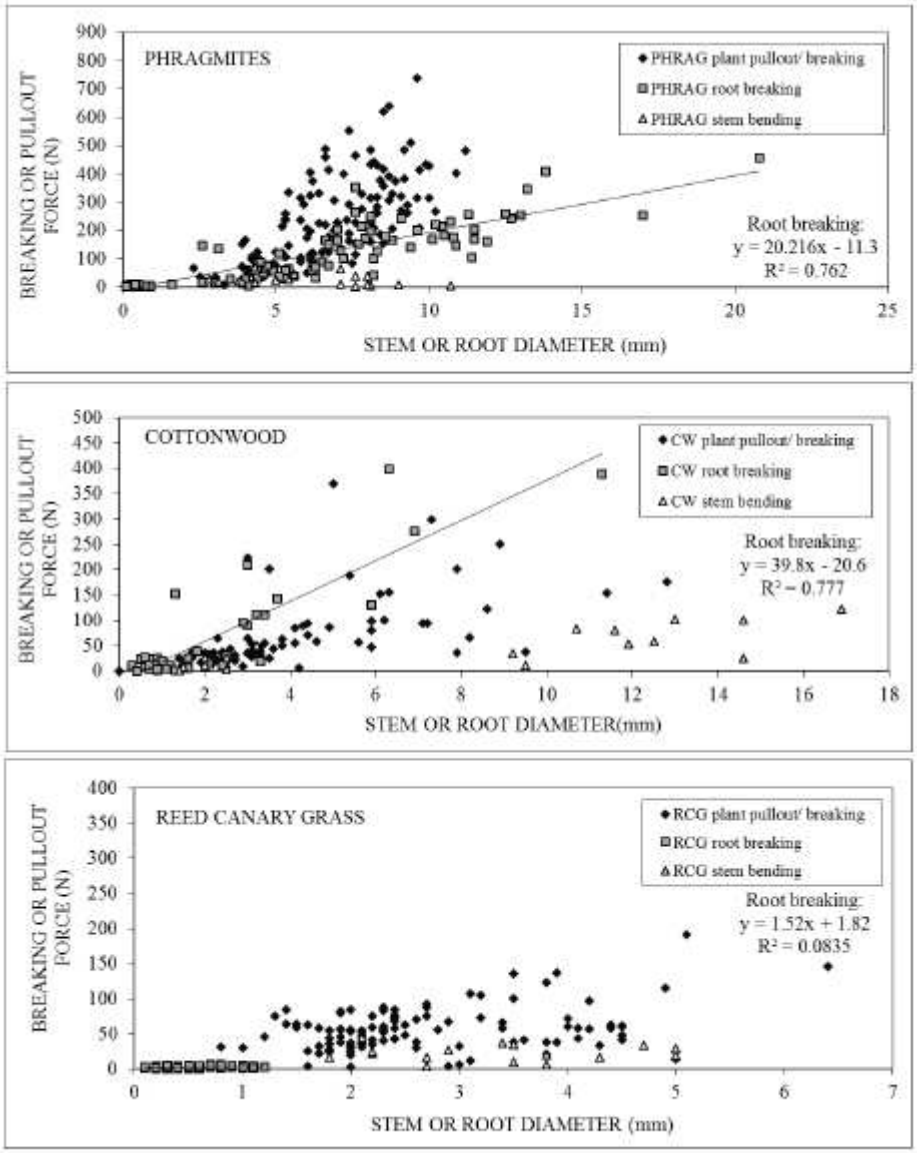

Figure 8. Plots comparing plant pullout forces with root breaking and stem bending forces.

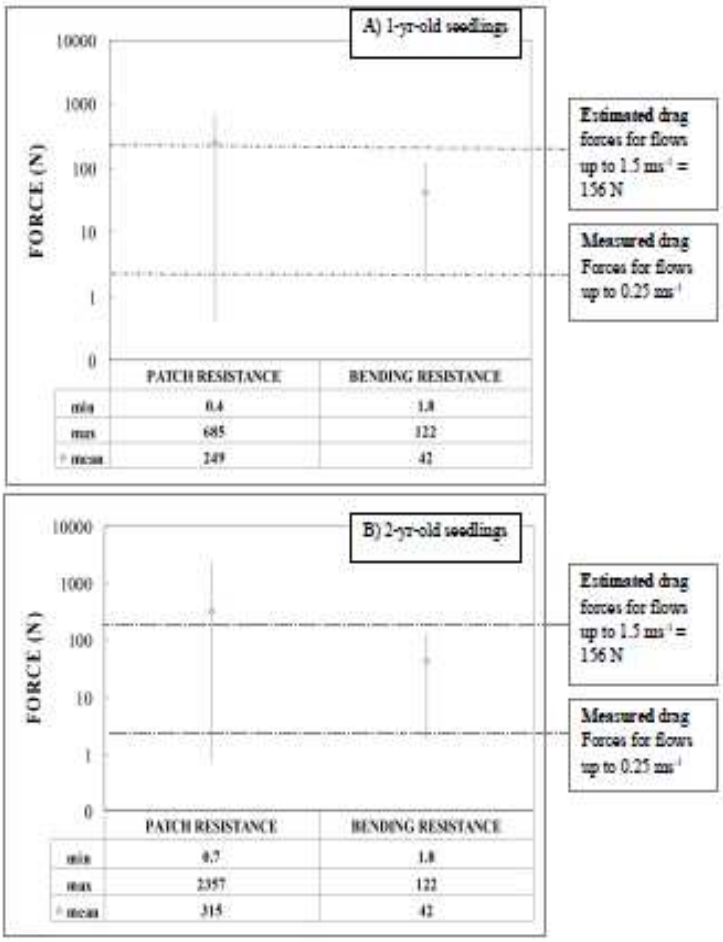

Figure 9. Maximum drag (driving) forces calculated from flume study, and estimated for maximum in-field velocities, compared with patch uprooting resistance, and bending resistance. A) shows results for 1-year-old cottonwood seedlings with stem density of 26 stems per m^2 and B) shows results for 2-year-old cottonwood seedlings with stem density of 13 stems per m^2. Drag forces acting on young cottonwood seedlings were calculated to be as high as 156 N at a flow velocity of 1.5 ms^{-1}, and would be sufficient to bend all young (<2 years old) cottonwood seedlings growing on sandbars. In addition, drag forces at 1.5 ms^{-1} are likely to be capable of removing the weakest one to two-year old seedlings. The estimated drag force acting at this velocity (156 N) is still well below the mean values for patch resistances of one and two year old cottonwood seedlings (249 and 315 N, respectively).

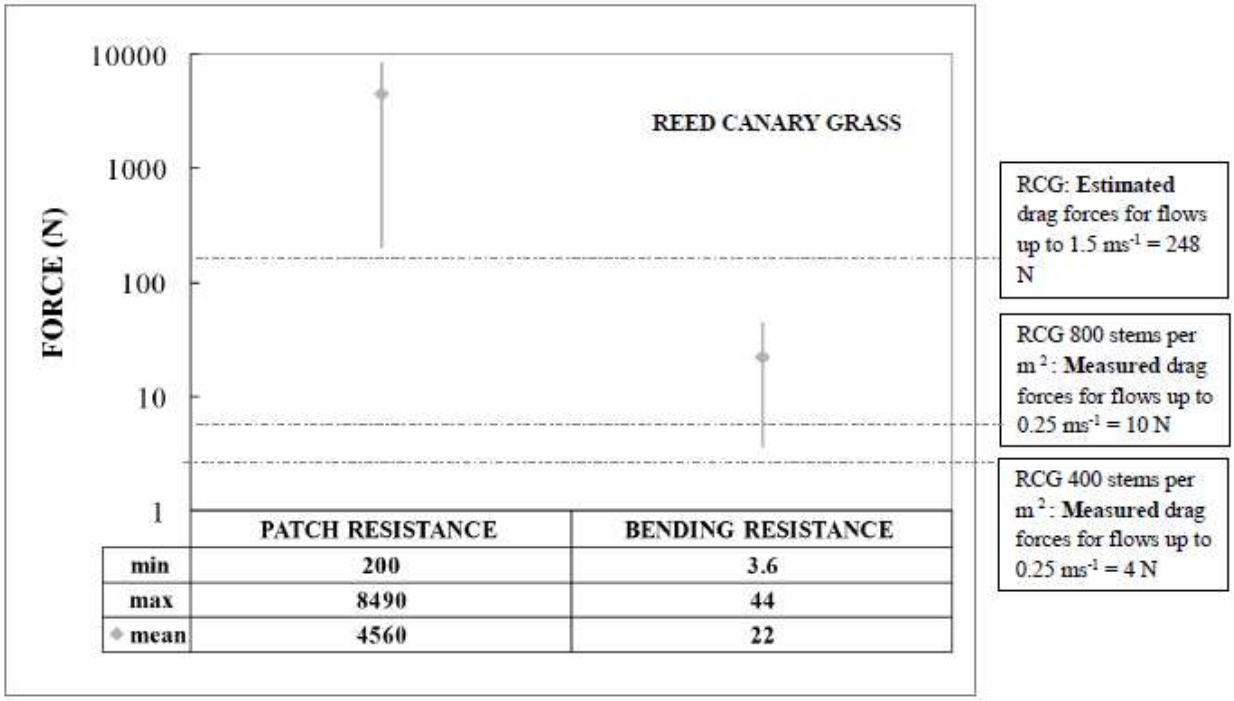

	PATCH RESISTANCE	BENDING RESISTANCE
min	200	3.6
max	8490	44
mean	4560	22

Figure 10. Maximum drag (driving) forces calculated from flume study, and estimated for maximum in-field velocities, compared with patch uprooting resistance, and bending resistance A) shows results reed canarygrass with a stem density of 400 stems per m^2 and B) shows results for reed canarygrass with a stem density of 800 stems per m^2.

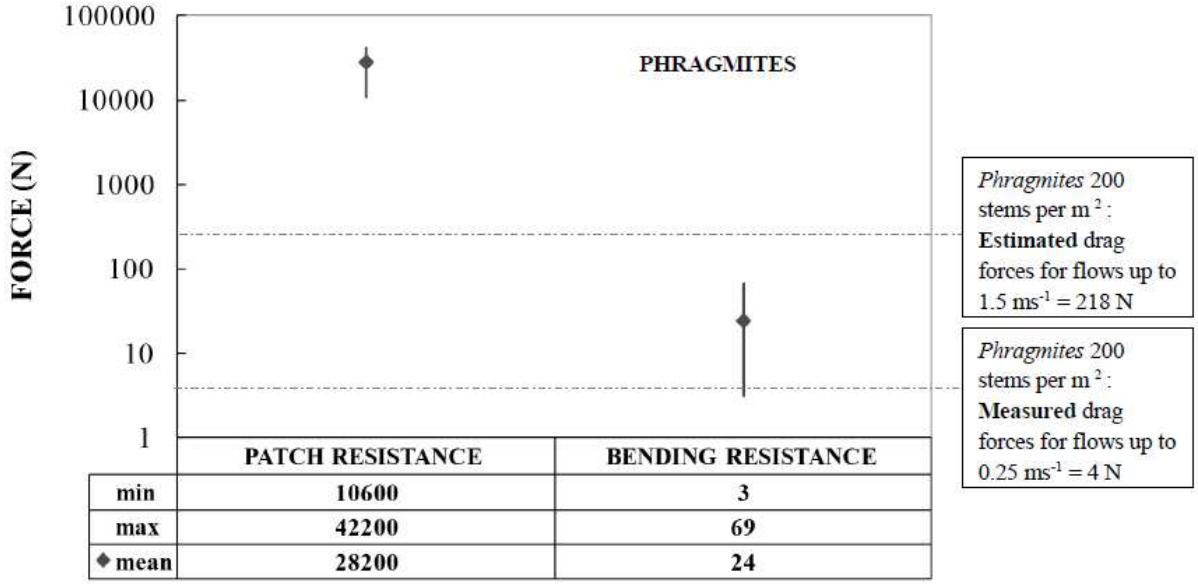

	PATCH RESISTANCE	BENDING RESISTANCE
min	10600	3
max	42200	69
◆ mean	28200	24

Figure 11. Maximum drag (driving) forces calculated from flume study, and estimated for maximum in-field velocities, compared with patch uprooting resistance, and bending resistance. Data shown are for *Phragmites* stems with a density of 200 stems per m^2.

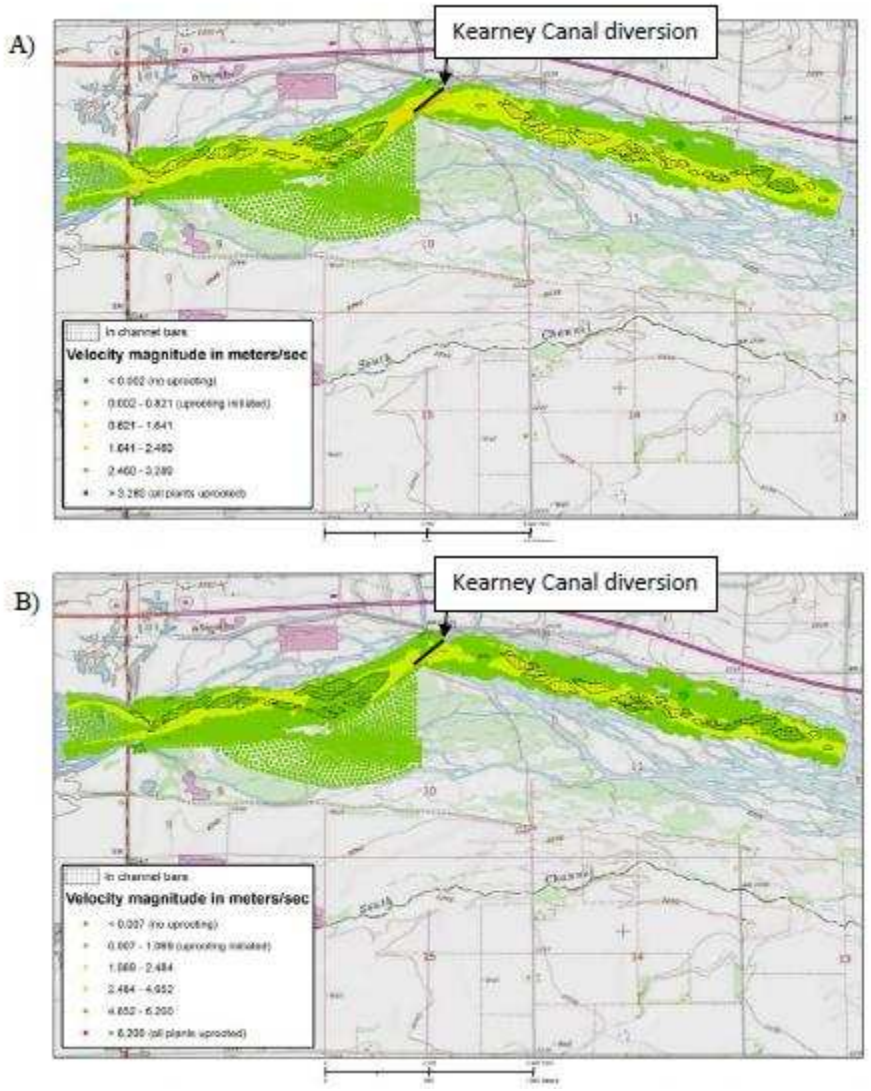

Figure 12. Velocities relating to the ability of drag forces to uproot patches of A) one-year old and B) two-year old cottonwoods during a 227 m^3s^{-1} flow event. Dark green areas indicate locations where velocities are so low that no uprooting of cottonwood seedlings would occur. The mid-green patches show where the weakest, most shallow rooted seedlings could be uprooted, with yellow and red velocity zones indicating the locations where velocities are high enough that uprooting is most likely, where these areas occur overlap with in-channel bars.

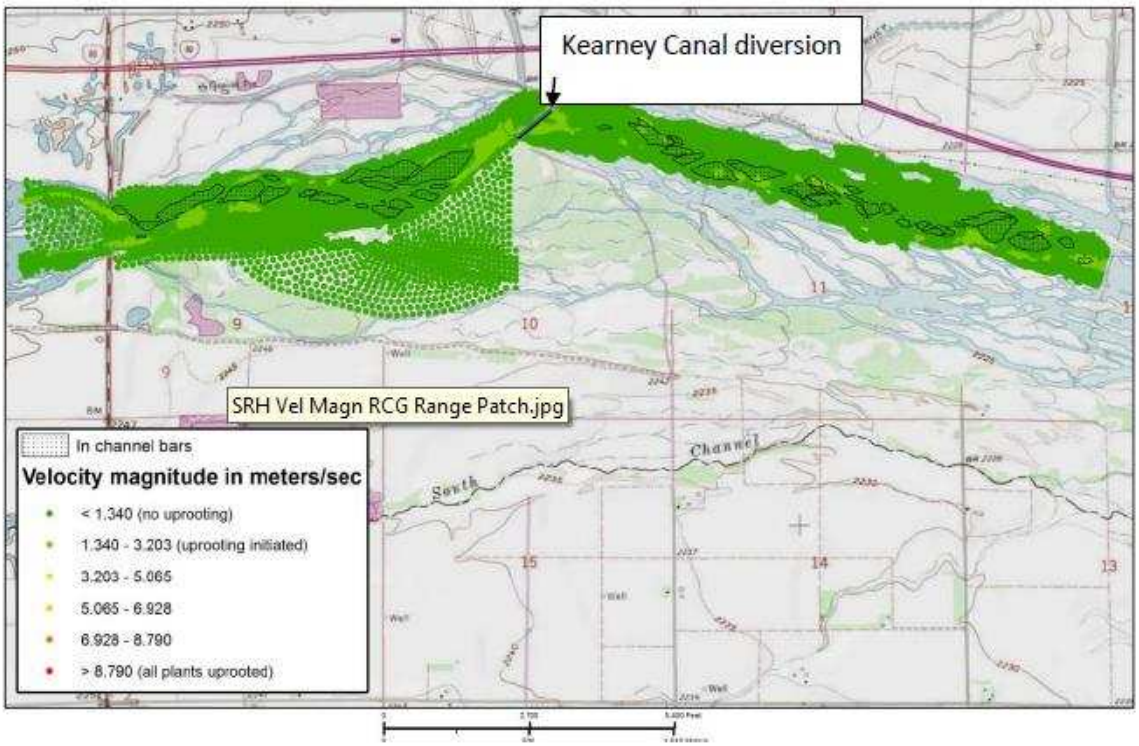

Figure 13. Velocities relating to the ability of drag forces to uproot patches of reed canarygrass during a 227 m^3s^{-1} flow event. Almost all parts of the channel are shaded in dark green, indicating that velocities are too low to remove even the weakest patches of grass in these locations. Areas of mid-green (indicating initiation of uprooting of the weakest stems) can be seen in some parts of the reach, but these correspond to deeper parts of the channel, rather than bars.

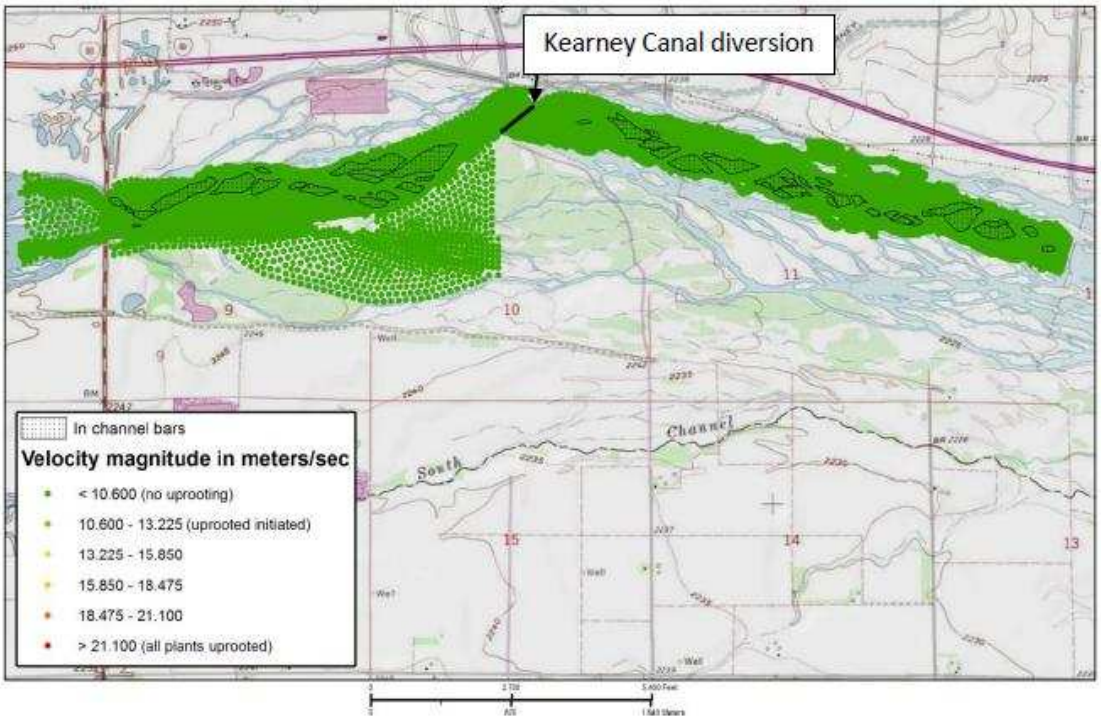

Figure 14. Velocities relating to the ability of drag forces to uproot patches of *Phragmites*. All zones are shaded dark green, showing no uprooting of *Phragmites* by drag is likely during a 227 m^3s^{-1} flow event.

Table 1. Results of field tests to measure flexural stiffness (presented as mean ± 1 standard deviation; note that distributions were positively skewed).

Species	Flexural stiffness, J ($N\ m^2$)	Number of Tests	Number of Evaluations
Cottonwood (Populus deltoides) seedlings (<3 years)	0.0099 ± 0.0082	10	23
Cottonwood (Populus deltoides) seedlings (3-5 years)	1.53 ± 1.86	10	80
Phragmites australis	0.94 ± 1.07	21	105
Reed canarygrass (Phalaris arundinacea)	0.18 ± 0.17	16	62

Table 2. Input parameters for RipRoot modeling.

Input Parameter	Cottonwood (Populus deltoides) (1 year old seedlings)	Cottonwood (Populus deltoides) (2 year old seedlings)	Phragmites australis	Reed Canarygrass (Phalaris arundinacea)
Minimum root/rhizome diameter (mm)	0.3	0.3	1.0	0.1
Maximum root/rhizome diameter (mm)	3.0	9.0	20.8	1.2
T_r a parameter*	15.05	15.05	16.2	3.63
T_r b parameter*	–0.52	–0.52	–0.91	–1.68
Minimum plant areal density (stems m^{-2})	1	1	96	348
Maximum plant areal density (stems m^{-2})	28	28	272	912
Substrate friction angle (°)	27.0	27.0	27.0	27.0
Substrate bulk density (kN m^{-3})	19.2	19.2	19.2	19.2
Maximum rooting length (m)	0.48	0.48	0.39	0.19
Number of roots/rhizomes failing by breaking	0 – 1	0 – 2	1 – 3	125
Number of roots/rhizomes failing by pullout	20	20	0	0

*Where root tensile strength equations are generally of the form $T_r = a\ D_r^{-b}$ and T_r = tensile strength (in MPa), D_r = root diameter (in mm), and a and b are regression parameters.

Table 3. Summary of drag coefficients and drag forces from flume study.

Species	Areal density, (stems m^{-2})	Drag coefficient from flume study at low discharge (0.0285 m^3s^{-1})	Drag coefficient from flume study at high discharge (0.0478 m^3s^{-1})	Drag force exerted on each plant at low discharge (0.0285 m^3s^{-1}) (N)	Drag force exerted on each plant at high discharge (0.0478 m^3s^{-1}) (N)
Cottonwood (Populus deltoides)	13	16.8 – 18.0	11.5 – 11.9	1.02 – 1.27	1.67 – 2.16
	26	11.9 - 16.9	13.2 – 15.5	1.07 - 1.28	2.22 – 2.47
Phragmites australis	200	8.81 – 13.0	7.27 – 10.8	1.20 – 1.78	2.78 – 4.13
Reed canarygrass (Phalaris arundinacea)	400	17.8 – 21.6	16.2 – 21.1	1.22 – 1.78	2.10 – 4.04
	800	10.4 – 15.8	9.73 – 13.1	1.41 – 2.16	3.72 – 5.00